USE OF ECMWF PRODUCTS IN STRATOSPHERIC MEASUREMENT CAMPAIGNS

A F TUCK
NOAA AERONOMY LABORATORY
BOULDER, COLORADO, USA

Summary: This paper reports some scientific highlights discovered during the STEP, AAOE and AASE missions with the ER-2 aircraft, and during the continuing operation of the HALOE instrument on the UARS satellite. ECMWF products were used in forecast mode during the AAOE, AASE and HALOE campaigns, and for analysis on all 4 missions. Successes, failures and questions concerned with the ECMWF forecast/analysis system are outlined.

1. INTRODUCTION

The NASA ER-2 is a modified version of the U2R reconnaissance aircraft, and is capable of flight at altitudes up to FL680 (50 hPa, 20·5 km) with a full polar payload, with a radius of action of some 24 great circle degrees during an 8-hour flight. In this paper, we report on water vapour and some meteorological data for 3 campaigns: The Stratosphere-Troposphere Exchange Project (STEP) tropical mission from Darwin (12°S, 131°E) in January - February 1987, The Airborne Antarctic Ozone Experiment (AAOE) from Punta Arenas (53°S, 70°W) in August - September 1987 and the Airborne Arctic Stratospheric Expedition (AASE) from Stavanger (59°N, 6°E) in January - February 1989. A fourth and rather different observational system has also been used; the Halogen Occultation Experiment (HALOE) on the Upper Atmosphere Research Satellite (UARS). Stratospheric observations of water vapour and methane (whose oxidation provides a source of water vapour in the middle and upper stratosphere) are described. Key results are reported, and some shortcomings in the forecast/analysis system noted.

2. STEP, DARWIN 1987

The observations of water vapour and total water (the sum of vapour and evaporated ice crystals) were made by the Lyman-α resonance fluorescence hygrometer of Kelly (*Kelly et al.*, 1989, 1993). The average profile of total water over Darwin during January and February shows, for the first time, that a location exists where the minimum in water (the hygropause) is spatially and temporally coincident with the minimum in temperature (the tropopause). This constitutes evidence that air enters the stratosphere in this region. The coincidence is not evident in earlier observations over Panama (9°N, 80°W), see Figure 1. A second result was that the upper troposphere was frequently saturated, and that the form of this saturation took the form of large populations of small ice crystals, see figure 2 (*Kelly et al., 1993*). A third result, due to *Danielsen* (1993) was that a continental scale anticyclone at 100 hPa plays a major role in the dehydration, see Figure 3. Note that the radiosonde temperatures at 90 to 100 hPa in Figure 3 on the

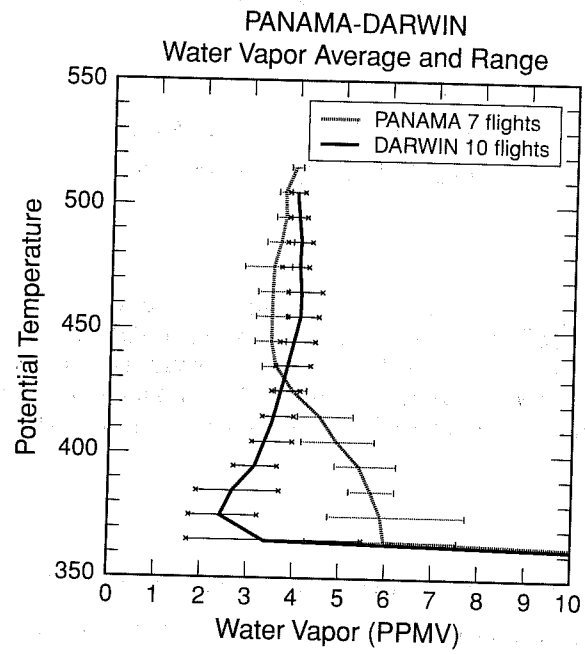

Fig 1 Average profiles of total water at Panama and at Darwin. At Panama, the hygropause is above the tropopause, at Darwin it is coincident with it.

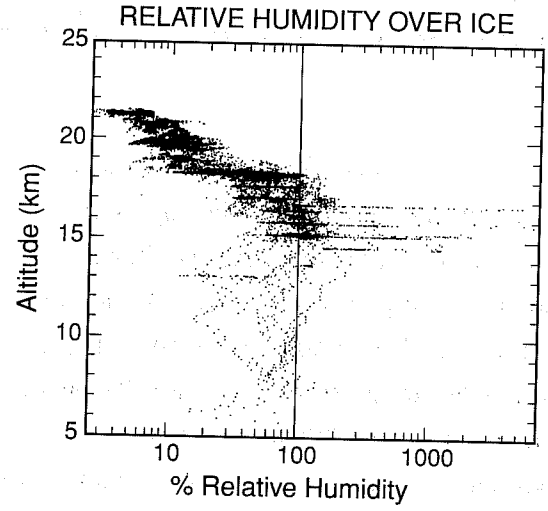

Fig 2(a) Relative humidity over ice, ER2 data from Darwin, Jan - Feb 1987.

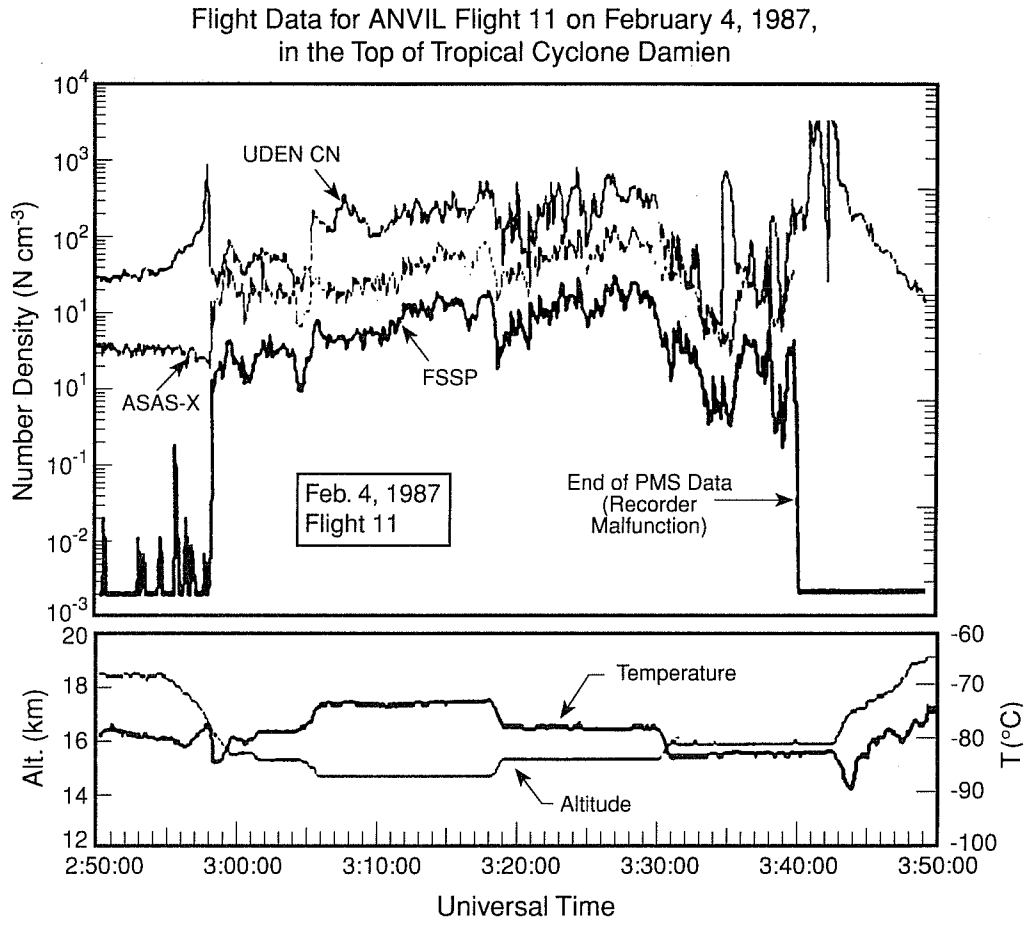

Fig 2(b) Particle number densities, ER2 flight of 870204 in an anvil. The closeness of the number of particles from the ice crystal instruments (ASAS-X, FSSP) on a logarithmic scale, to the total number of particles (UDEN CN) indicates that most of the ice is in the form of large numbers of small particles.

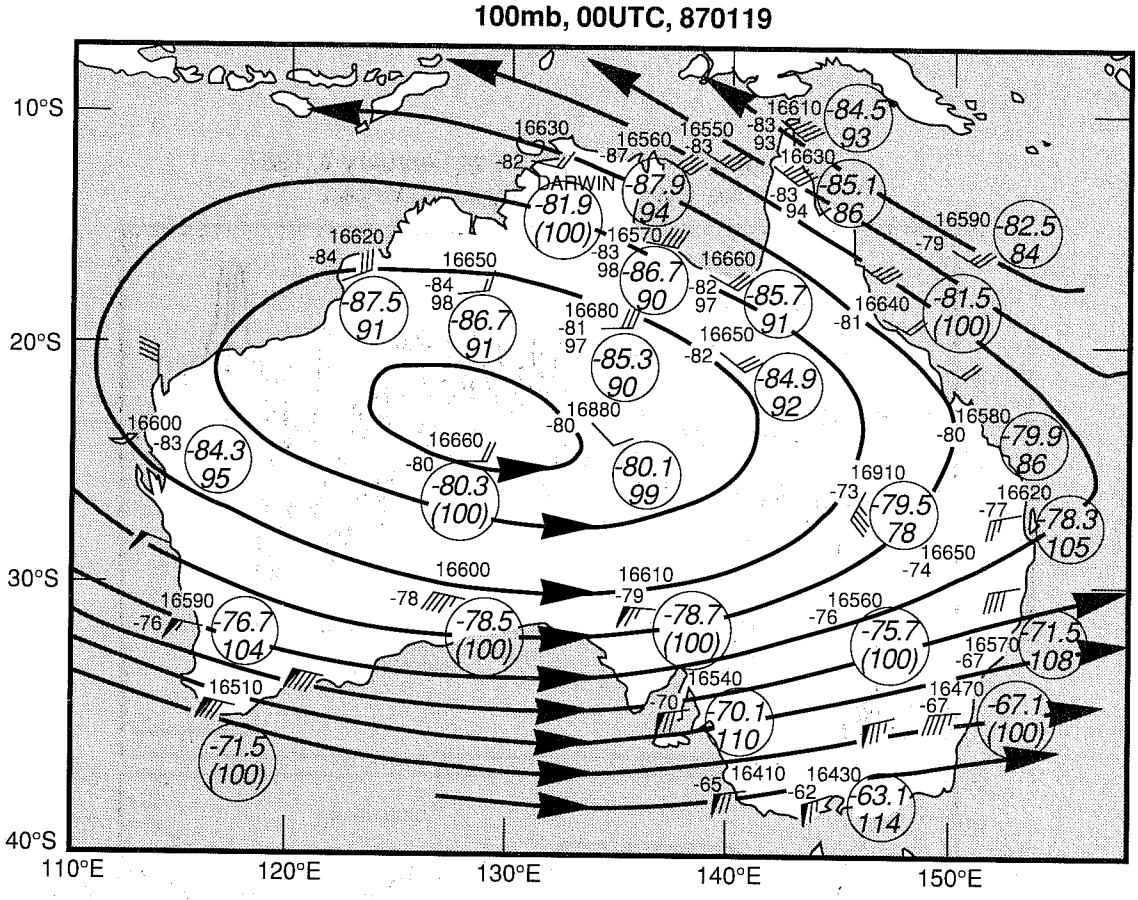

Fig 3 Australian area 100 hPa analysis, 870119, OO UT. The larger, circled numbers near each radiosonde station indicate the minimum temperature (deg C) observed by the sonde and the pressure (hPa) at which it occurred. Note that this continental scale circulation corresponds to a tilt in the isentropic surfaces such that air travelling equatorward will be adiabatically cooled to frost point temperatures consistent with the stratospheric water vapour content in 2 (a).

northern edge of the anticyclone are quantitatively in accord with the measured water vapour mixing ratios, and are in agreement with the aircraft temperature measurements. These temperatures, as low as –88°C, are several degrees colder than any temperatures which appear on the 100 hPa ECMWF analysis (see Figure 4 for an example). It will therefore be difficult for the model, if employed in free-running "GCM" mode, to correctly simulate the dryness of the stratosphere. Note from Figure 4 that the operational analysis (Figure 4a) is warmer than the analysis with the newer T213L31 model which also assimilated the AMEX data (Figure 4b).

3. AAOE, PUNTA ARENAS, 1987

The outstanding result from AAOE in a meteorological sense was the dryness of the Southern Hemisphere lower stratosphere, both inside and outside the vortex. Figure 5 illustrates this by means of vertical profiles, and Figure 6 shows all ER-2 water vapour data taken during four missions from 90°N to 72°S. The dryness of the Southern Hemisphere is very evident, and has been interpreted as indicating significant flux of dehydrated air from the Antarctic vortex to middle latitudes during austral winter (*Kelly et al.*, 1989, *Tuck*, 1989, *Kelly et al.*, 1990). Vertical profiles at the edge of the vortex show a pronounced laminar structure (Figure 7), and there is evidence for "peel-off" of dehydrated air in horizontal flight (Figure 8). Some trajectories initialized at PV = –33 (just inside the vortex) at Θ = 435 K using ECMWF assimilations during August 1987 clearly show some of these air parcels leaving the vortex for lower latitudes (Figure 9). This figure also shows air parcels from the vortex edge penetrating deep into its centre over east Antarctica. One shortcoming noticed during this campaign occurred often during the period; when an upper tropospheric/lower stratospheric ridge system pushed poleward over West Antarctica, particularly in the Antarctic Peninsula/Weddell Sea sector, the amplitude and wind speeds were underestimated and the temperatures overestimated (see Figure 10). Since these events are responsible both for the forcing of polar stratospheric clouds and exchange at the vortex edge (*McKenna et al.*, 1989, *Tuck*, 1989), there are important stratospheric consequences; this is evident in the analysis as well as the forecast, since in this data sparse region the forecast tends to become the analysis. The UK Met O analysis was also inadequate during these events (*Salter and Merrick*, 1989).

4. AASE, STAVANGER, 1989

The Arctic during the winter of 1988/89 reached frost point temperatures only briefly in the vortex, and the vortex air at ER-2 flight altitudes had higher water vapour mixing ratios inside it than outside, because of the descent of methane - poor air from aloft in the vortex. In contrast to the Antarctic, the Arctic vortex has therefore high rather than low mixing ratios of water vapour, compared to its environs. There were clear examples of the shedding of filaments of vortex air. We show two here, one of which was well reproduced by the ECMWF PV analysis, one of which was under-represented. Figure 11 shows tracer, wind and potential temperature observations along the aircraft track for 890106 at Θ = 420 K. The ECMWF analysis (Figure 12) shows very well the observed split structure of the polar night jet stream over Scandinavia, and

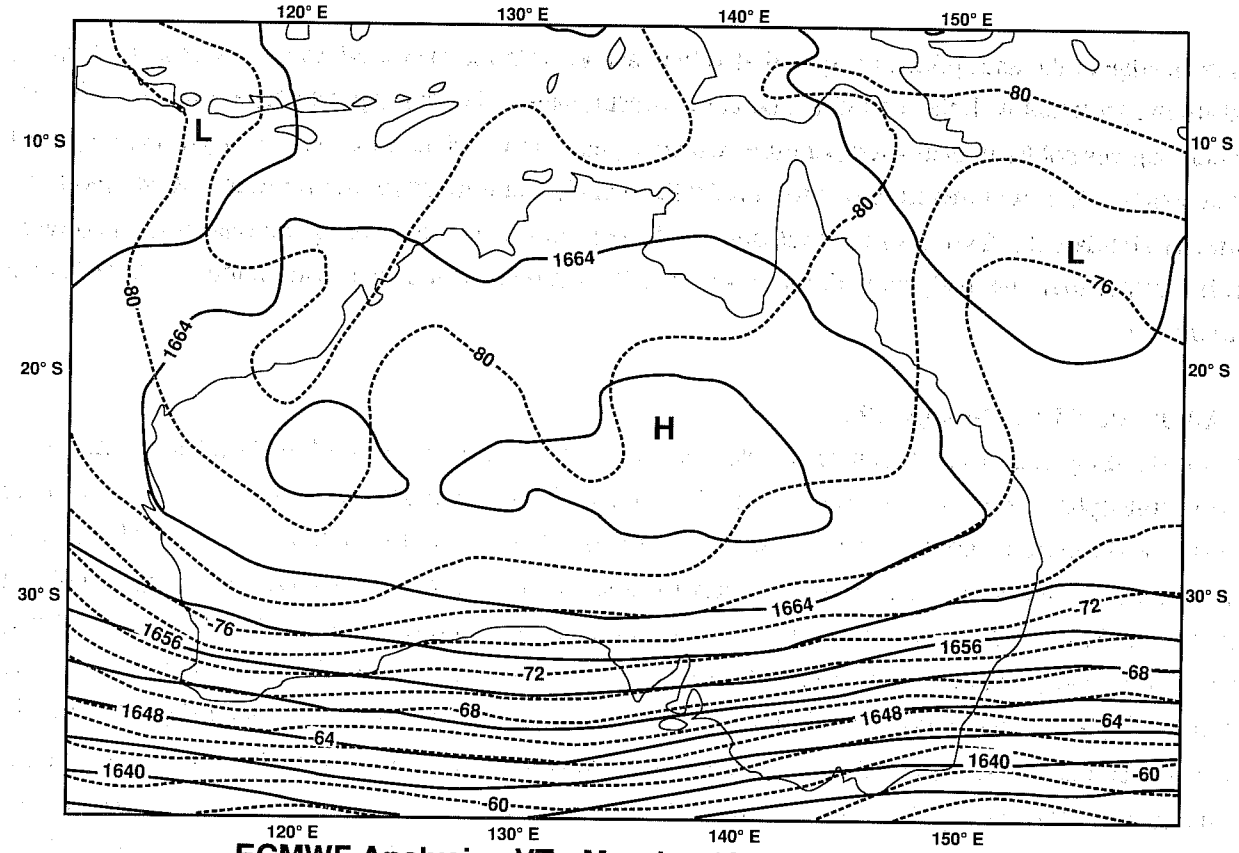

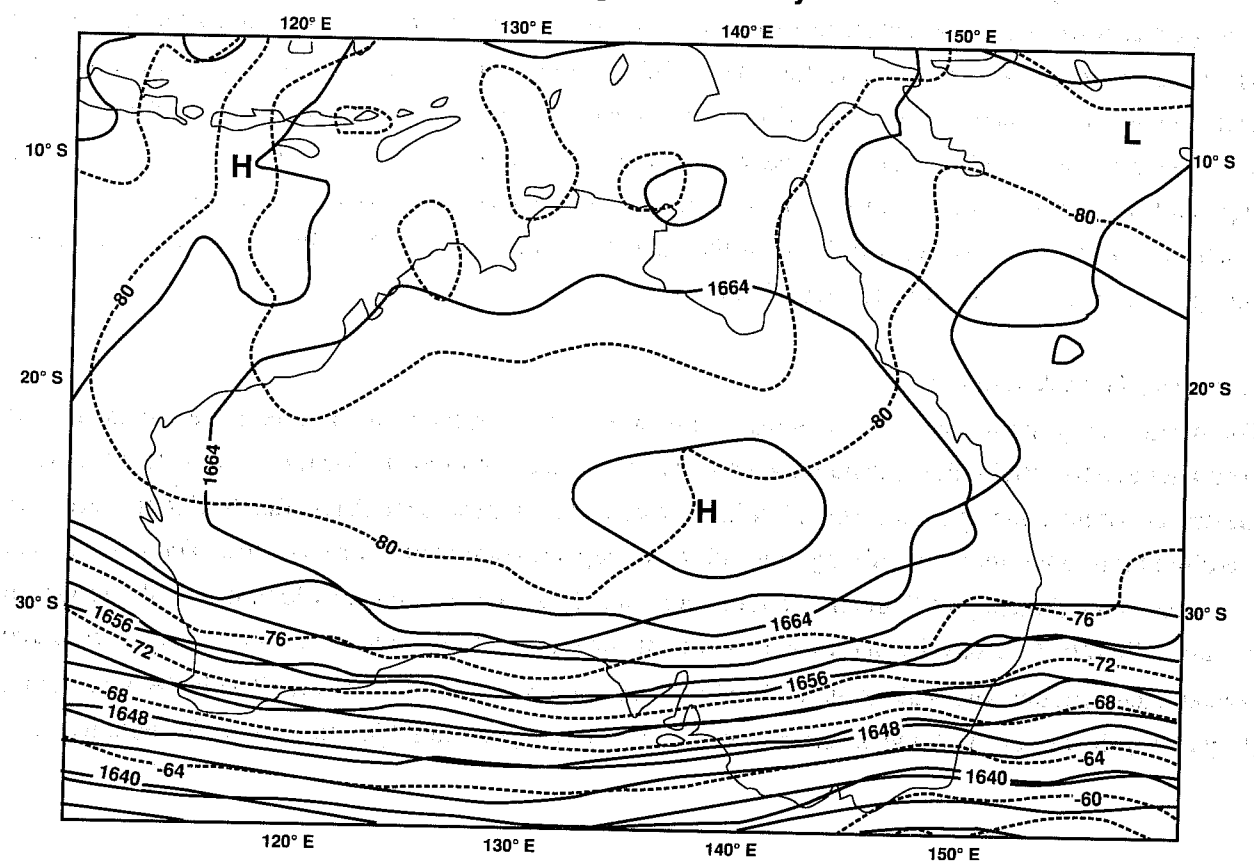

Fig 4 ECMWF analyses, 100 hPa, 870119. Compare with Fig 3: (a) operational analysis, (b) new analysis incorporating AMEX data. Although the new analysis is an improvement, the temperatures are still too warm compared to observations.

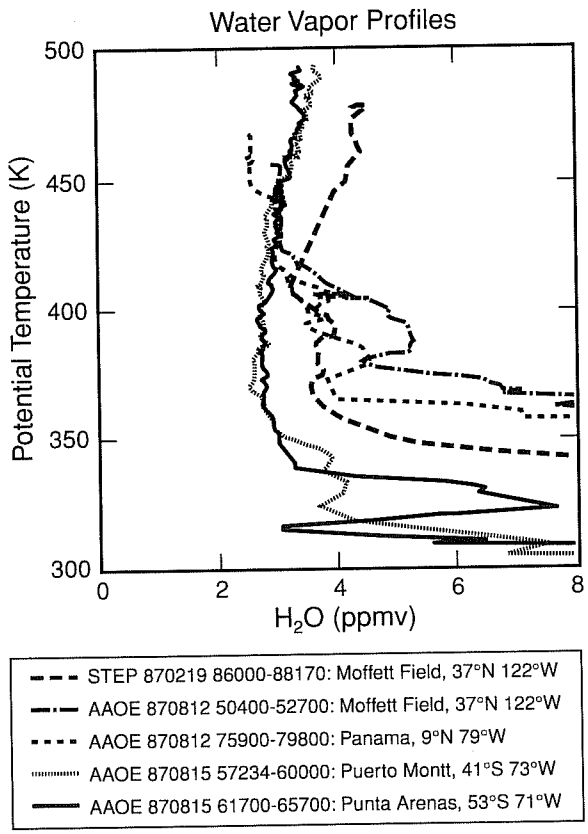

NOTE: Data are 15 second average

Fig 5 Vertical profiles of water taken during 1987. Note that the northern hemisphere and tropical profiles are consistent with each other and with figures 1 and 2(a), but that the southern hemisphere profiles, which are outside the vortex, are not. Both as regards amounts and shape, they are consistent with temperature and humidity profiles inside the Antarctic vortex.

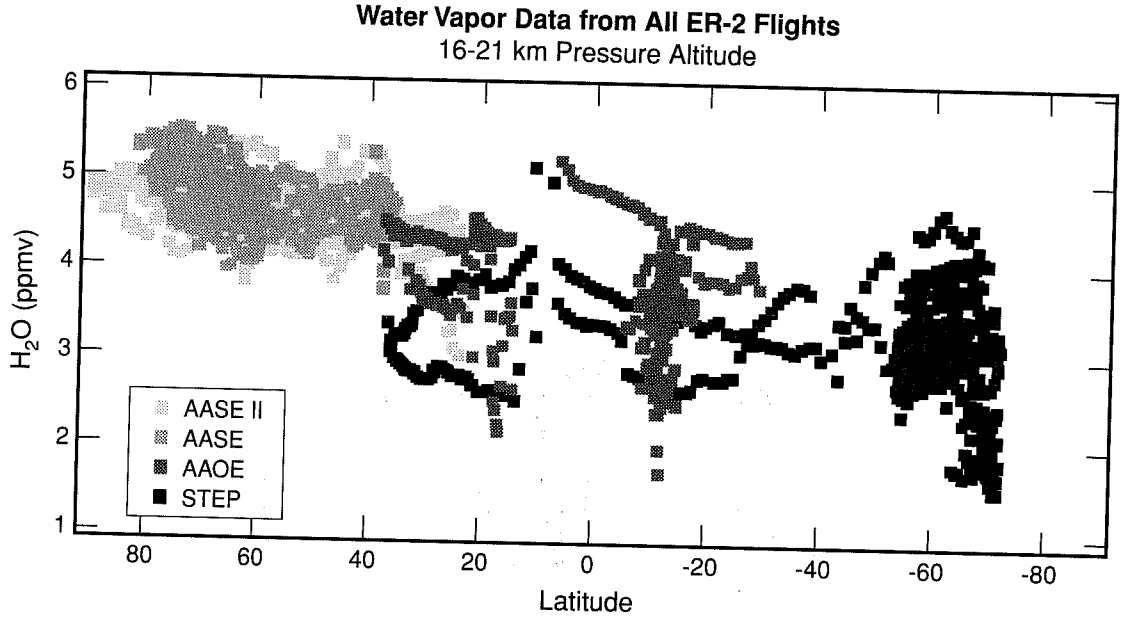

NOTE: Each point represents a 5 minute average.

Fig 6 Water data taken by the Lyman-α resonance fluorescence hygrometer on the ER2 during the STEP-Tropical, AAOE, AASE and AASE missions. Note that the lower stratospheric slope in mixing ratio is from 90° N to 72° S, with some low values near Darwin during northern winter.

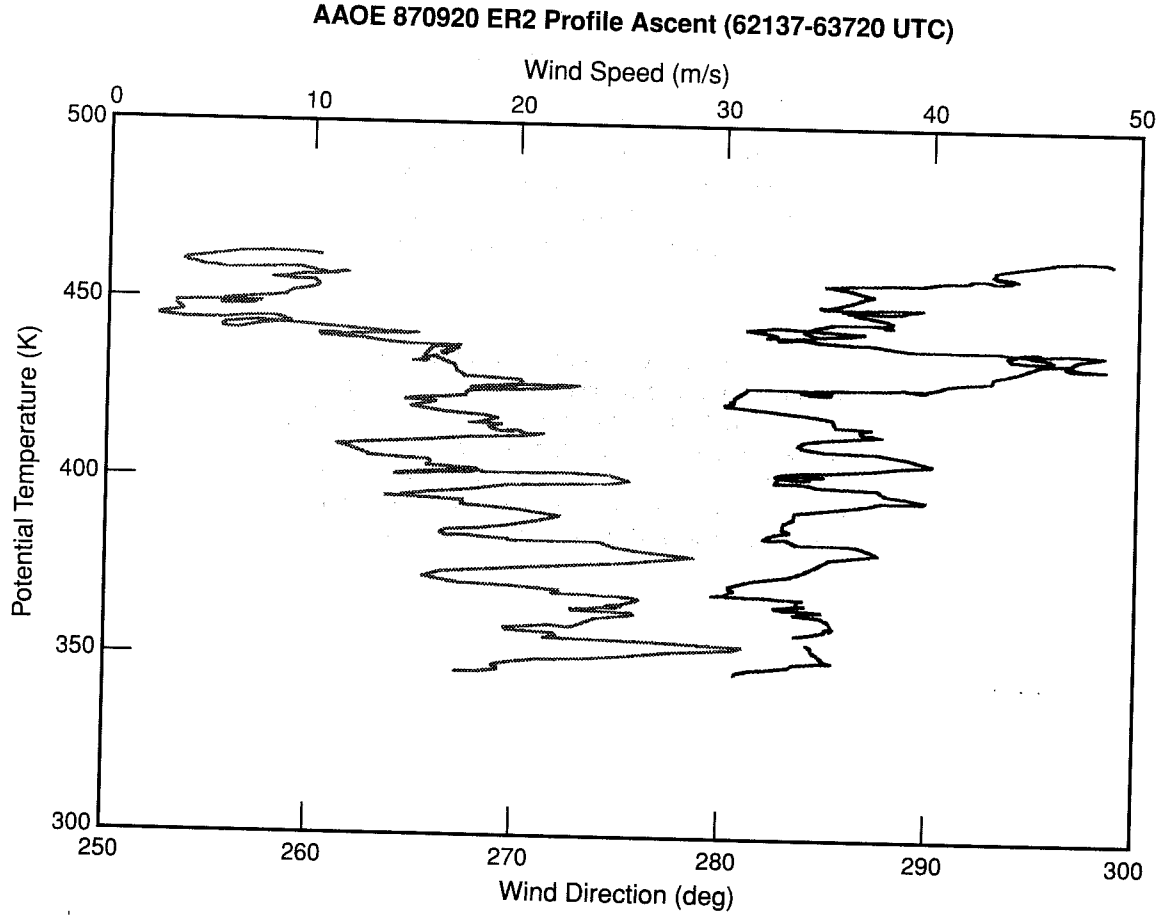

Fig 7 Laminar structures in a vertical profile at the core of the austral polar night jet stream. Note that laminae occur in wind speed, wind direction and in molecular species; flight date was 870920.

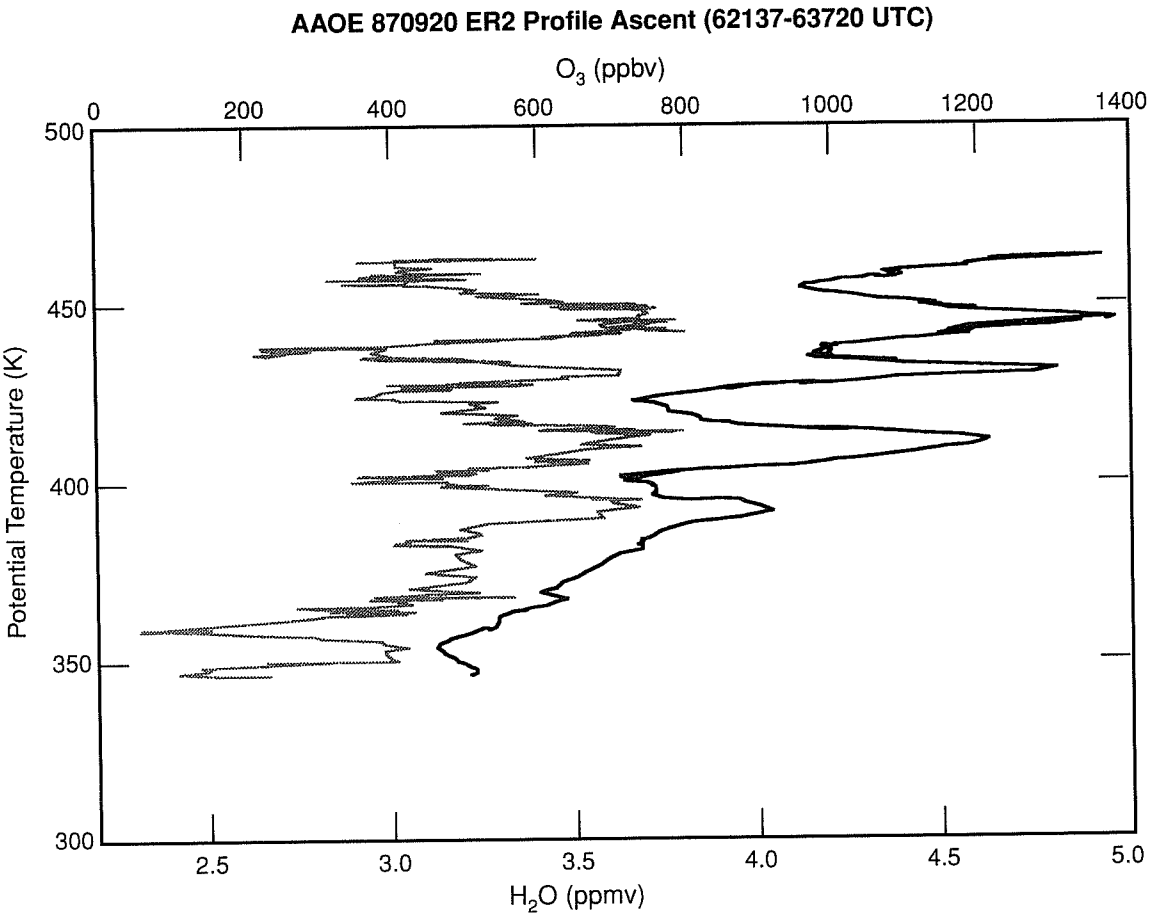

Fig 7 (continued) Laminar structures in a vertical profile at the core of the austral polar night jet stream. Note that laminae occur in wind speed, wind direction and in molecular species; flight date was 870920.

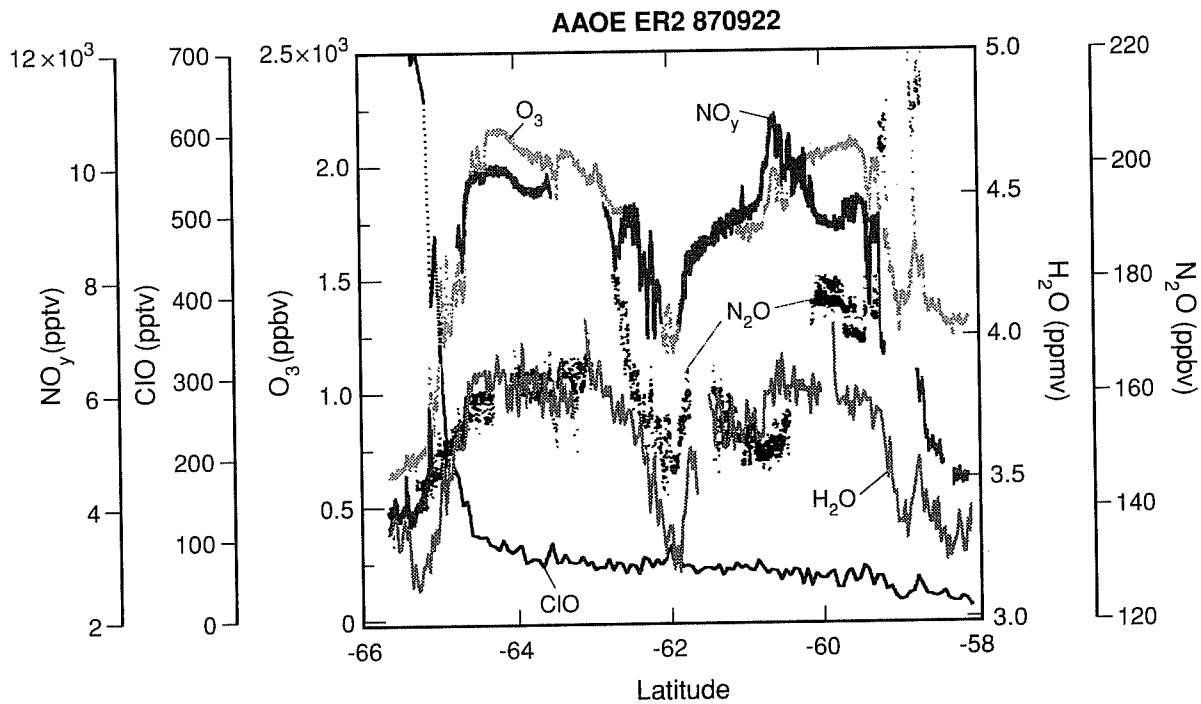

Fig 8 The vortex edge at Θ = 425 K, the isentropic level of this ER2 flight on 870922, is at 65°S, where ClO rises and O_3, NO_y, N_2O and H_2O drop. The air between 61° and 63°S has been peeled from the vortex; the ClO, a reactive free radical, has been lost by recombination with NO_2 in the intervening interval. The low N_2O in this filament (~ 150 ppbv) indicates that the air did not come from equatorward of 59°S, where N_2O is greater than 200 ppbv.

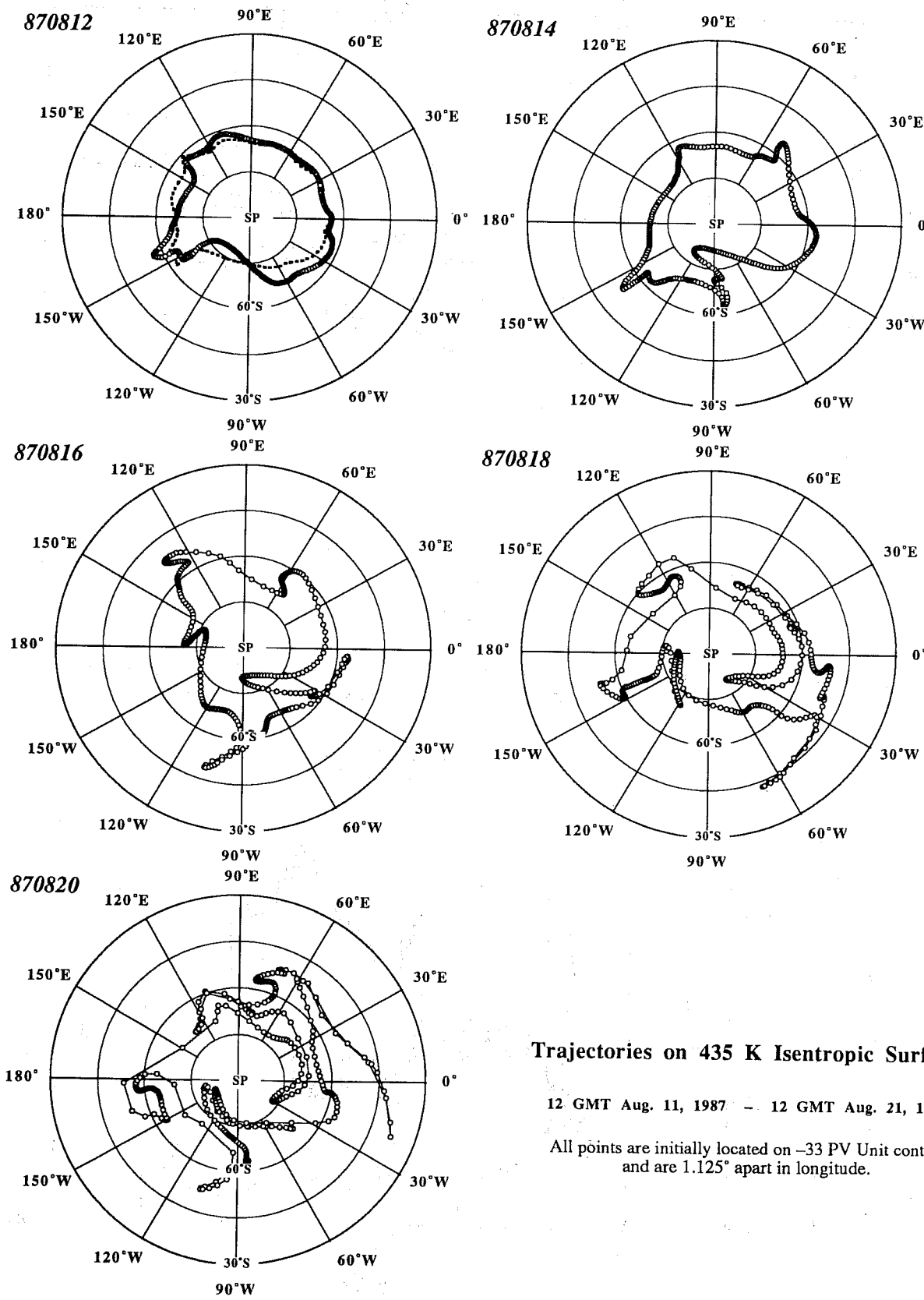

Trajectories on 435 K Isentropic Surface

12 GMT Aug. 11, 1987 – 12 GMT Aug. 21, 1987

All points are initially located on –33 PV Unit contour and are 1.125° apart in longitude.

Fig 9 The 10-day behaviour of a ring of air parcels started with PV = -33 at Θ = 435 K on 870812, inside the vortex. By 870816, filaments have left the vortex; low PV air has entered it over East Antarctica by 870818.

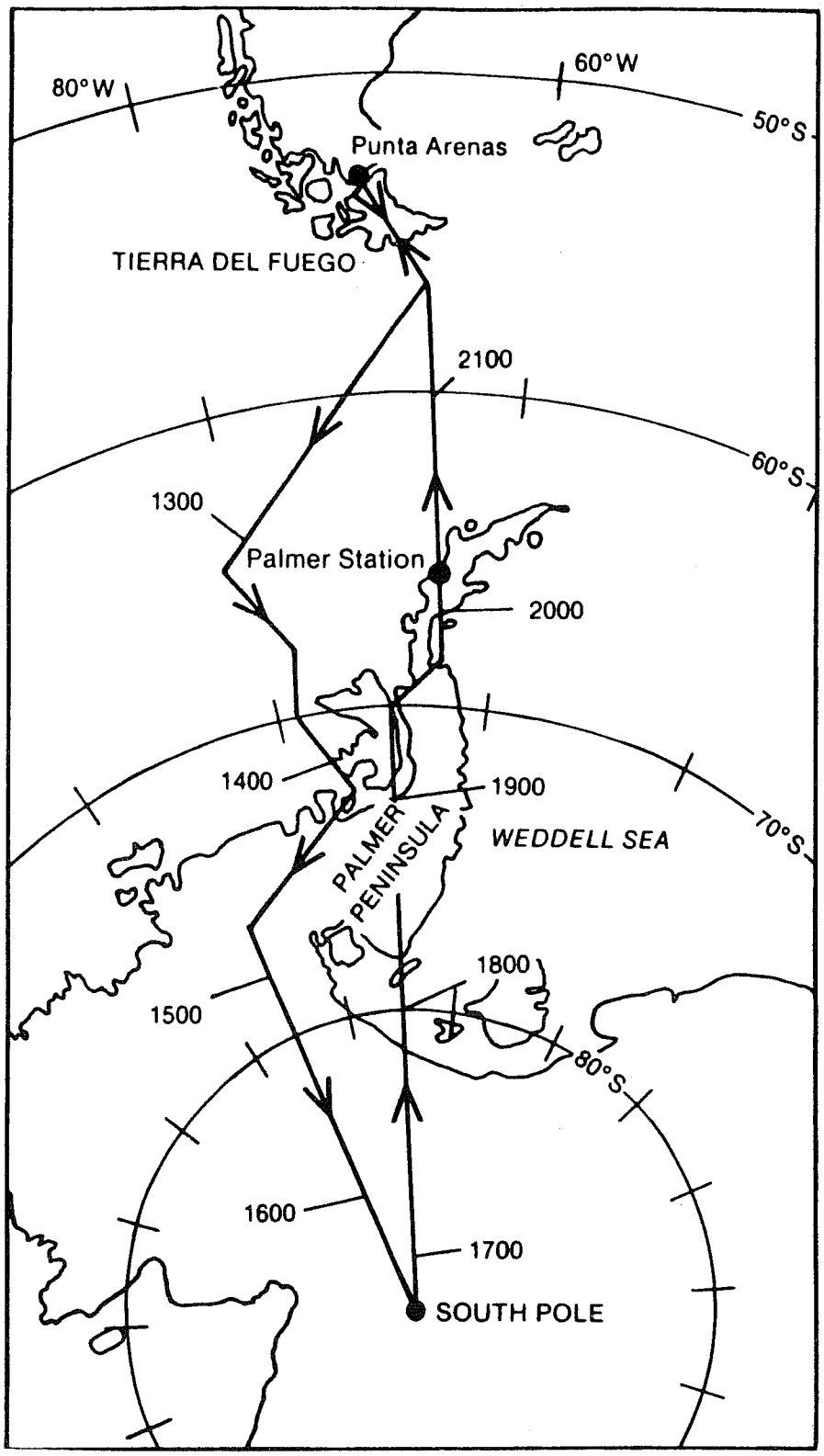

Fig 10 (a) DC8 flight track over Antarctica, 870902 at approximately FL 340 (about 250 hPa).

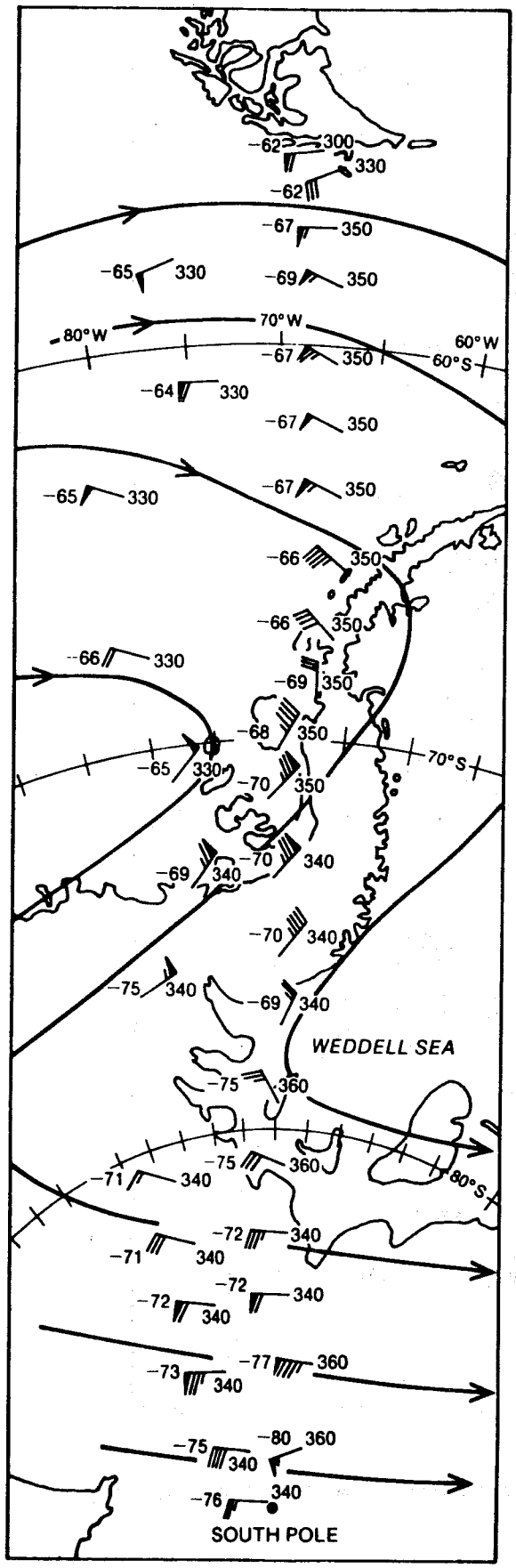

Fig 10 (b) Observations of temperature with flight level made from the DC8.

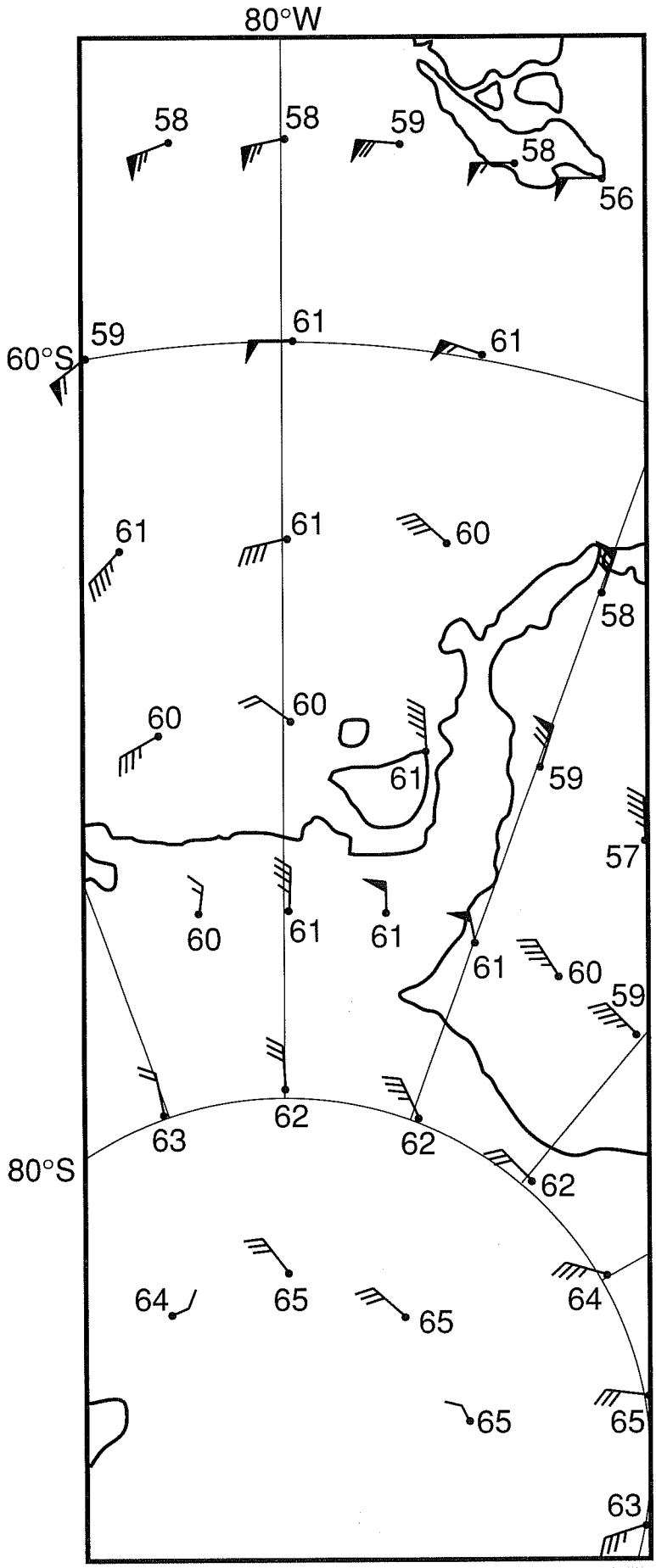

Fig 10 (c) T + 24 ECMWF forecast, 870902, 250 hPa. Winds are underestimated, the ridge morphology and amplitude are wrong compared to Fig 10(b), and the temperatures are too warm.

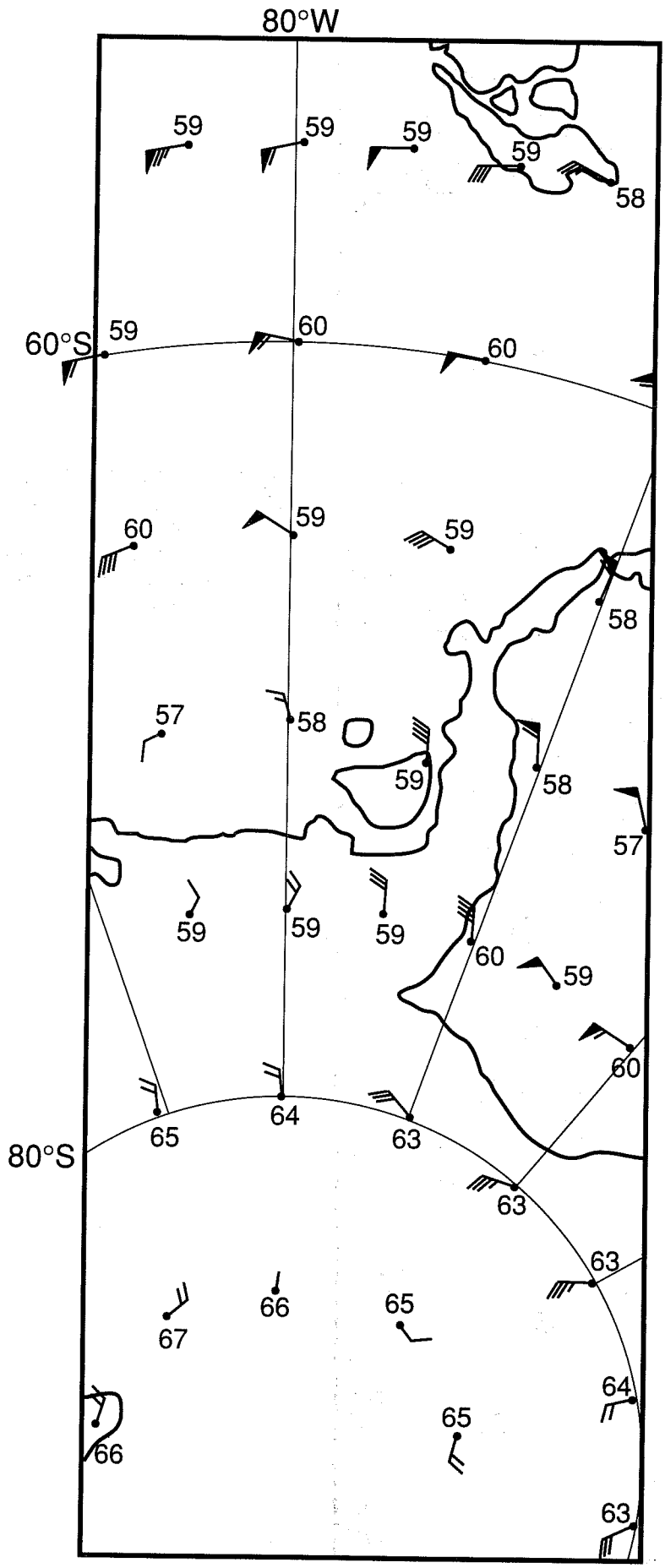

Fig 10(d) T + 00 ECMWF analysis, 870902, 250 hPa. Winds are underestimated, the ridge morphology and amplitude are wrong compared to Fig 10(b), and the temperatures are too warm.

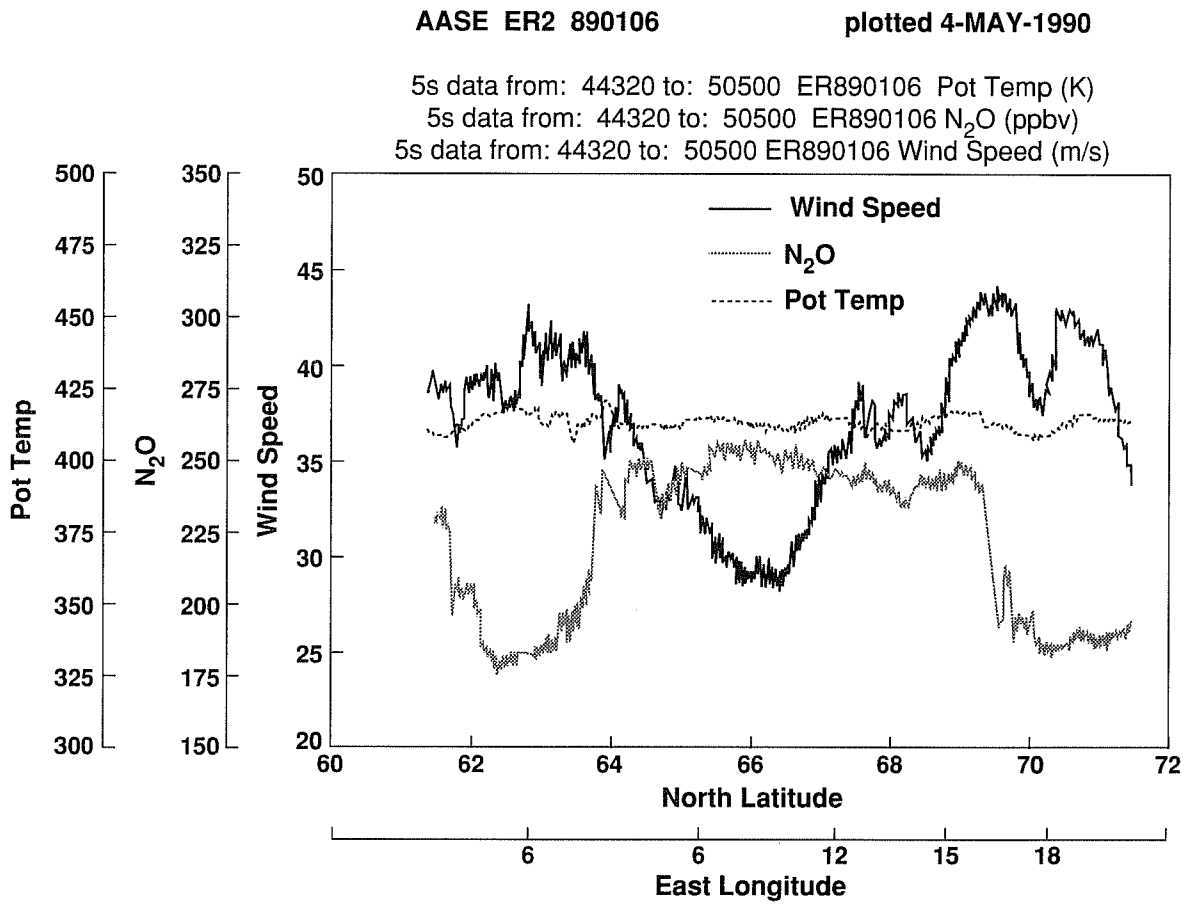

Fig 11 Wind speed, potential temperature and N_2O tracer along an isentropic section of ER-2 flight track on 890106. Note the good agreement of the winds with the ECMWF analyzed wind field in fig 12, and the peeled-off vortex air 61° - 64°N. The vortex edge is at 69·5°N.

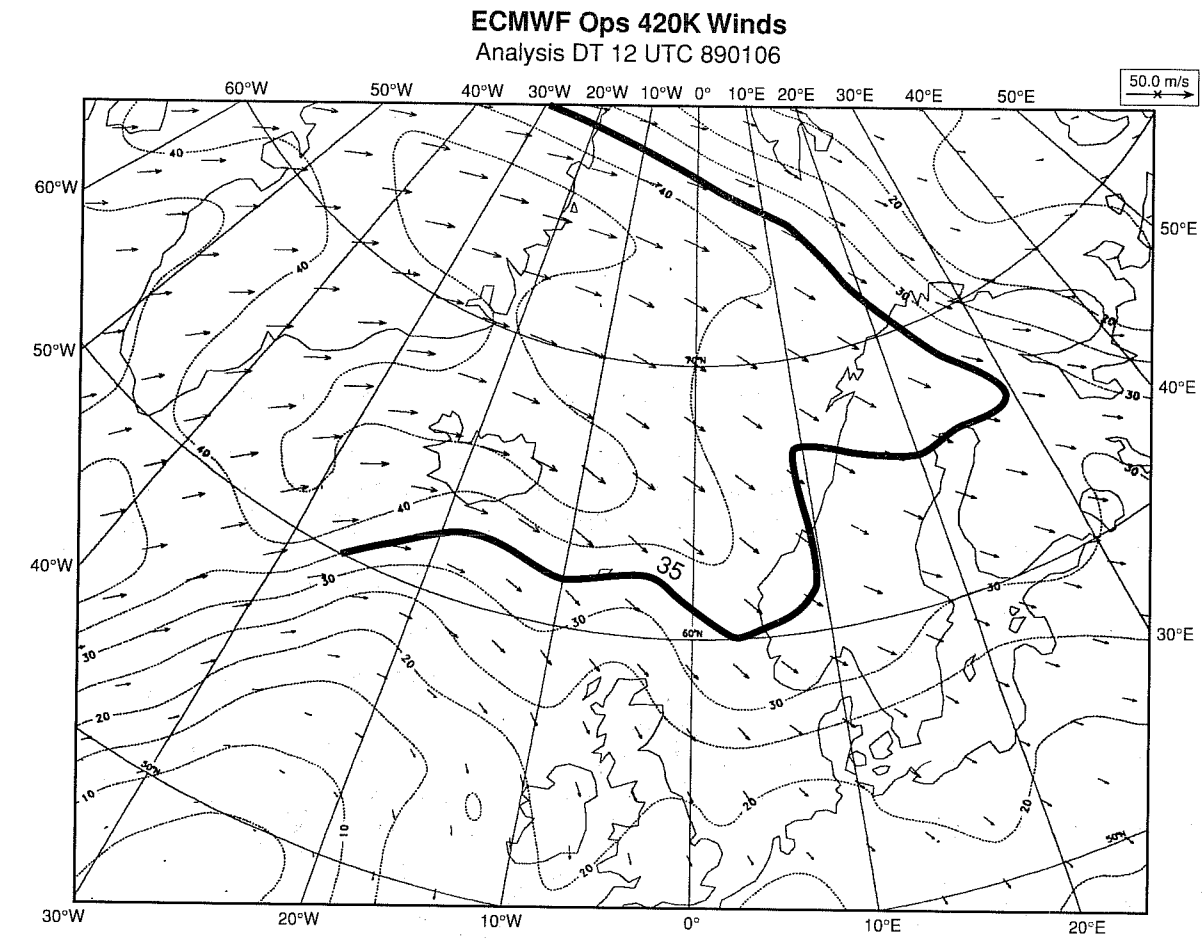

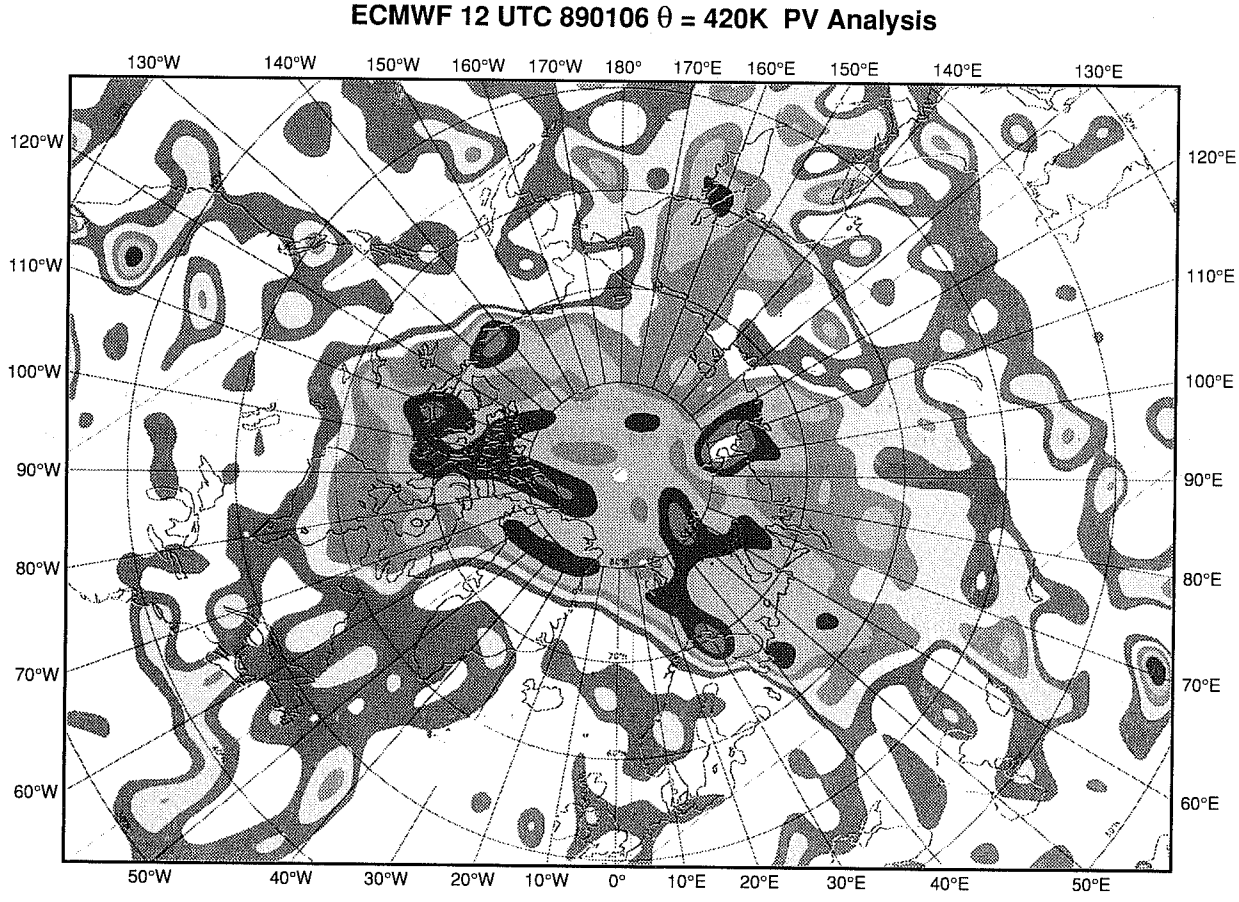

Fig 12 ECMWF analysis, (a) winds at Θ = 420 K, 890106. Compare with observations in fig 11; (b) PV at Θ = 420 K. The position of the ex-vortex air over Scandinavia agrees well with the N_2O tracer observations in Fig 11.

the PV analysis has a piece of ex-vortex air in the same location as the aircraft observations show it, co-located with the equatorward of the two wind maxima. On this same day, a vertical profile at the jet core revealed the laminar structure at the edge of the vortex (Figure 13). Note that this profile occurs above a tropopause fold extending downwards to the mid-troposphere (Figure 14).

The flight of 890220 from Stavanger to Wallops Island (38°N, 75°W) approximately paralleled the vortex edge, and revealed a considerable amount of filamentary structure, showing vortex air peeled off from the edge (*Tuck, et al.,* 1992). Figure 15 shows these results; Figure 16 shows ECMWF PV maps for the day, at varying resolutions from analyses and at T63 for the T + 24 forecast. The forecast shows no trace of the observed structure, and even the analysis underestimates its extent: there are 2 crossings of ex-vortex air implied by the PV analysis between 0°W and 40°W at 55°N - 60N, whereas at least six were observed, with other concomitant small-scale structure. These observations suggest that at least some of the ubiquitous features with PV characteristic of the vortex edge seen on analyses poleward of 25°N are in fact real, even if inadequate resolution makes what are probably filaments look like blobs. Some evidence that the blobs located over the main land masses in the subtropics, just poleward of and higher than the core of the sub tropical jet stream maxima are real is provided by trajectory analysis; back trajectories from the blobs themselves invariably go back to the edge of the vortex on a 5 to 10 day time scale, those from the low PV air surrounding them remain in the subtropics (Figure 17). Thus, if these subtropical high-PV features are artefacts, they are advected in a self-consistent manner after they are created at the vortex edge. Although there is no aircraft evidence in these subtropical locations, we shall see that there is satellite evidence that suggests that vortex edge air is deposited in the subtropics.

A further result from AASE at Stavanger was that clouds there at and even just above the tropopause were frequent, much more so than above Punta Arenas (*Murphy, et al.,* 1990). This is illustrated in Figure 18. It may be a reflection of Stavanger's location at the end of the storm track associated with the Gulf Stream, or it may be more general - the interhemispheric difference may arise because of a shortage of condensable vapour in the Southern Hemisphere, as a result of freeze drying over Antarctica.

5. HALOE, UARS, OCTOBER 1991 - PRESENT

The HALOE instrument measures the vertical profiles of 8 eight atmospheric species - CO_2, O_3, H_2O, and NO_2 by radiometry, HCl, HF, NO and CH_4 by gas correlation spectroscopy - in absorption by solar occultation at the limb (*Russell et al.,* 1993a). The results briefly reported here focus on the H_2O and methane, CH_4; to a useful appproximation, simultaneous measurements of these two molecules in the stratosphere are related by $D = 2 * CH_4 + H_2O$, where $D \approx 6{\cdot}5$ ppmv in those parts of the stratosphere where no precipitation of ice crystals has been experienced since entry through the tropical tropopause over the western tropical Pacific during northern winter. The oxidation of one methane molecule yields two water molecules, to an adequate approximation. The air entering the stratosphere seems to have on average 3·1 ppmv of water vapour and 1·7 ppmv of methane. The results from HALOE are consistent with the aircraft results, showing that the Southern Hemisphere lower stratosphere by the end of austral winter is

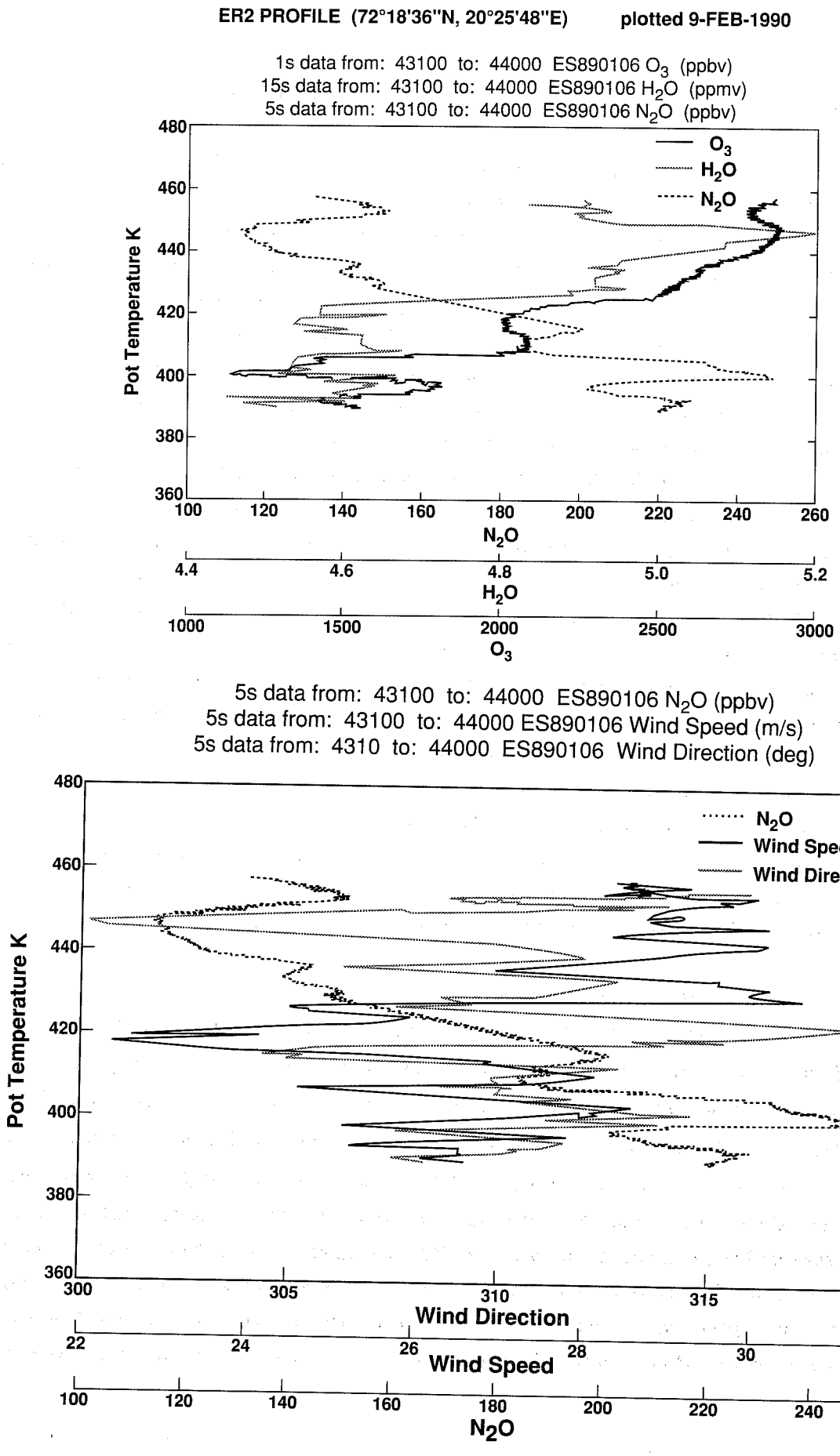

Fig 13 Vertical profile, 890106, same flight as figs 11 and 12. The profile was taken at the core of the coreal polar night jet stream, and shows laminae in molecular mixing ratios (a) and in wind speed and direction (b). Compare with fig 7.

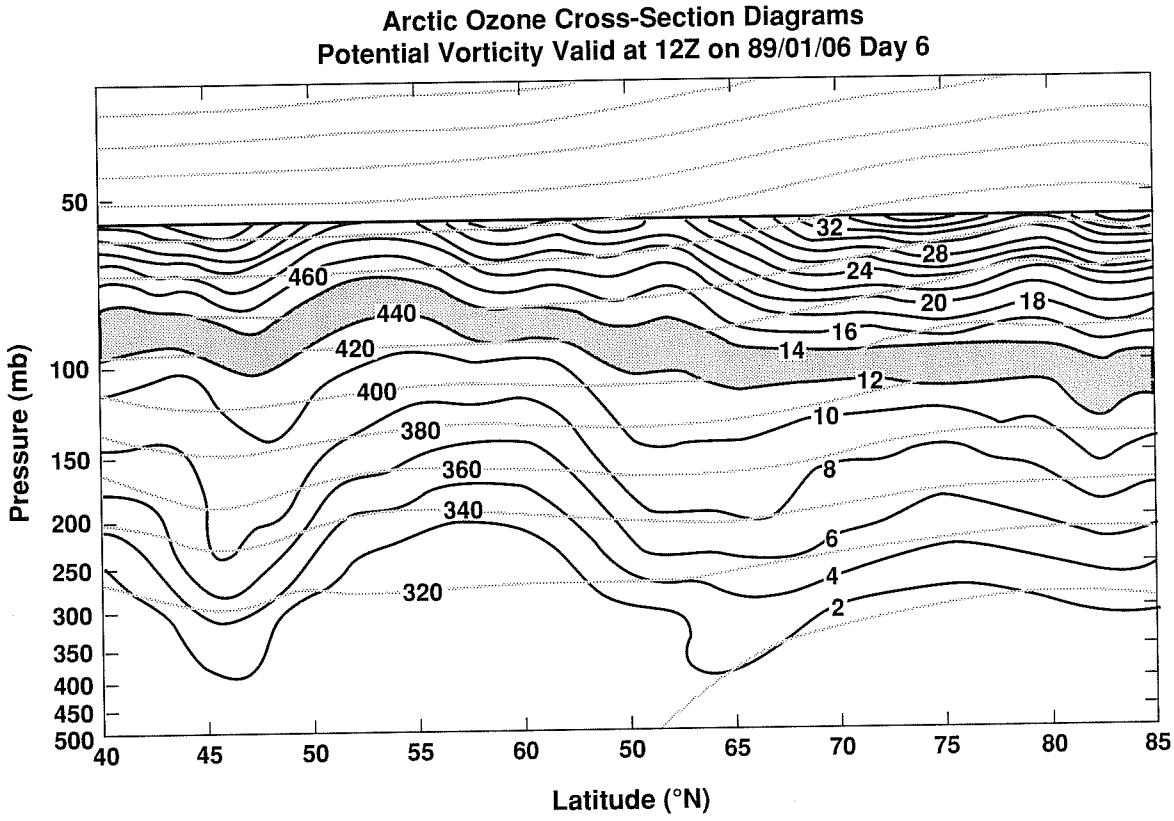

Fig 14 UKMO cross section of PV and Θ along the Greenwich meridian, 890106, the same day as figs 11, 12 and 13. Structures at Θ = 420 K in those figures are correlated with the structures in the upper troposphere.

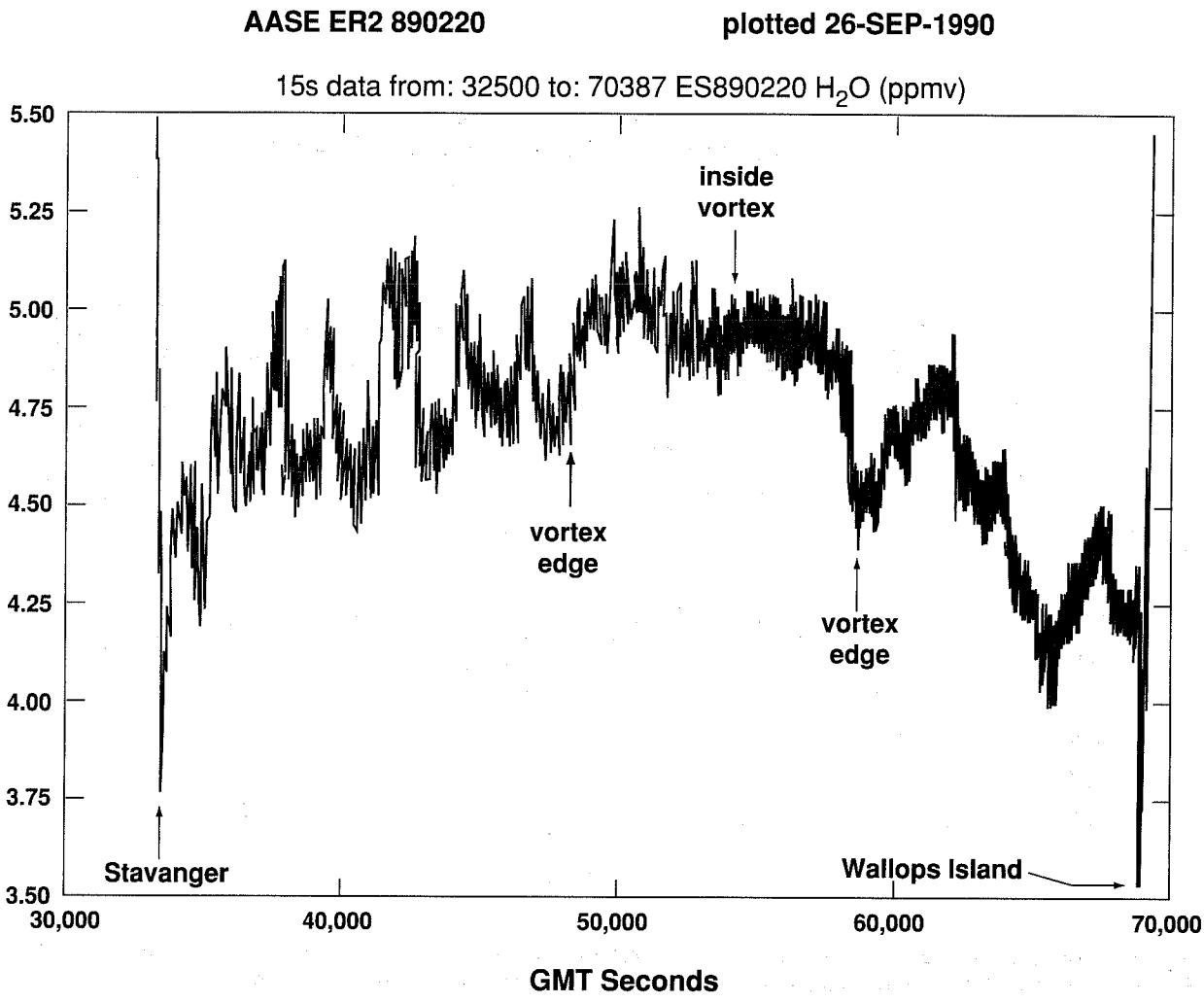

Fig 15 (a) Water vapour along the flight track of 890220, which is shown relative to the PV field at Θ = 475 K in (b). There are at least 6 filaments of ex-vortex air outside the vortex. The ER2 flew at 200 ms^{-1} ($\approx$ 400 knots).

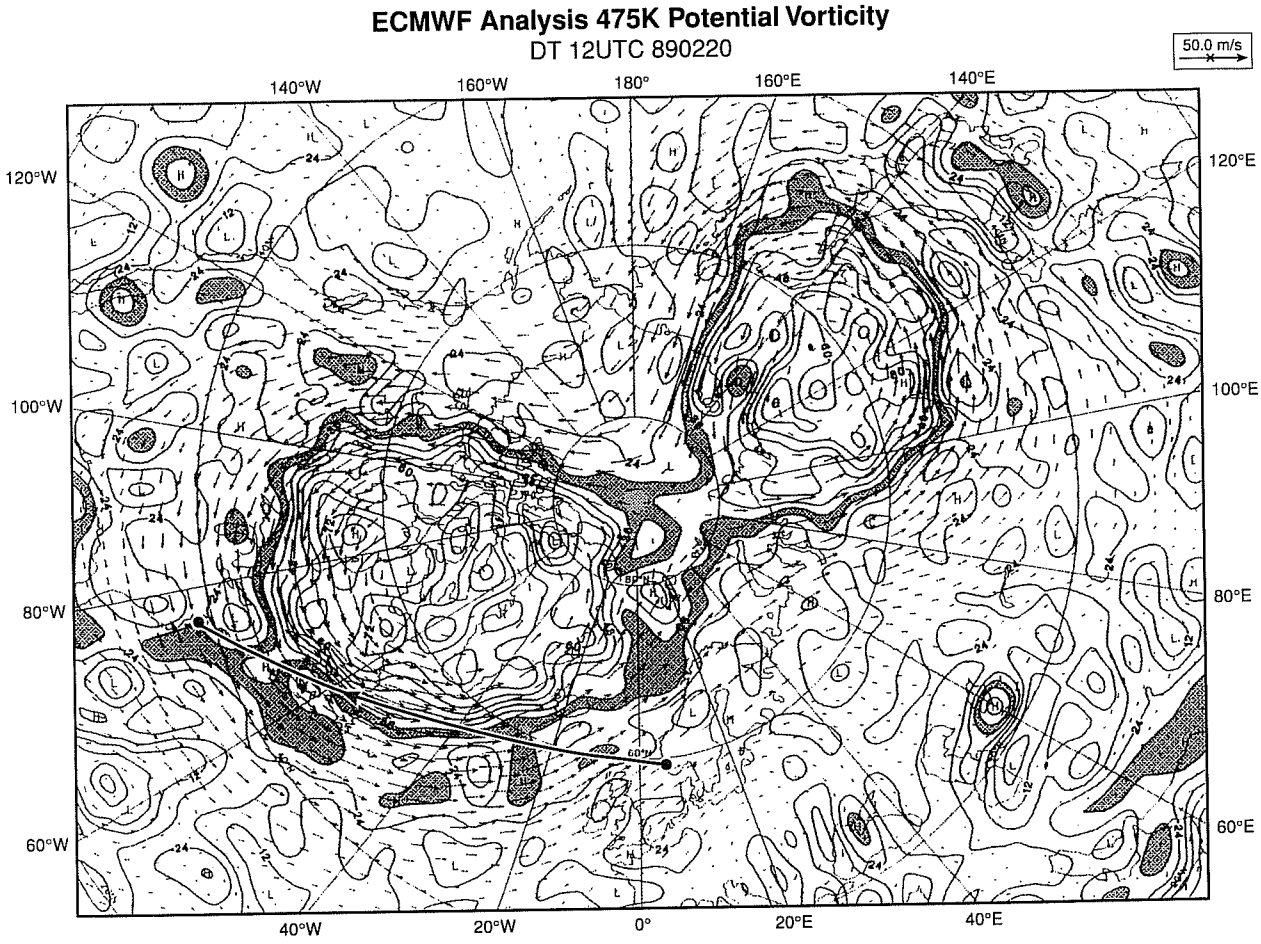

Fig 15(b) ER2 flight track, Stavanger - Wallops Island, relative to vortex edge. PV = 30 - 36 units shaded.

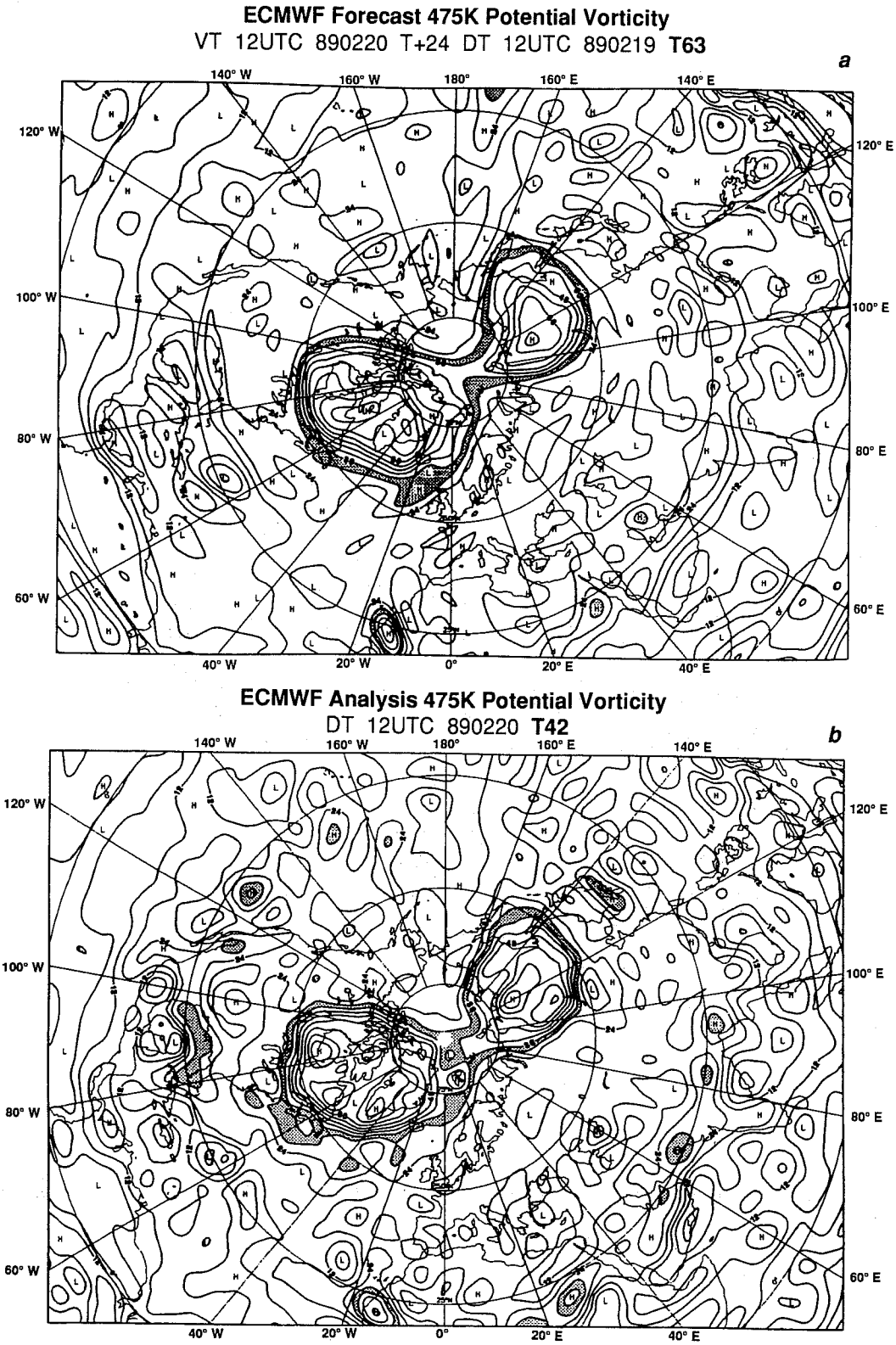

Fig 16 ECMWF PV maps for 890220, the day the observations in fig 15 were taken. (a) T + 24 forecast, T63; (b) T42 analysis; (c) T63 analysis; (d) T106 analysis. (a) and (b) are far too smooth; (c) and (d) are almost identical, and under-represent the observed structure in fig 15.

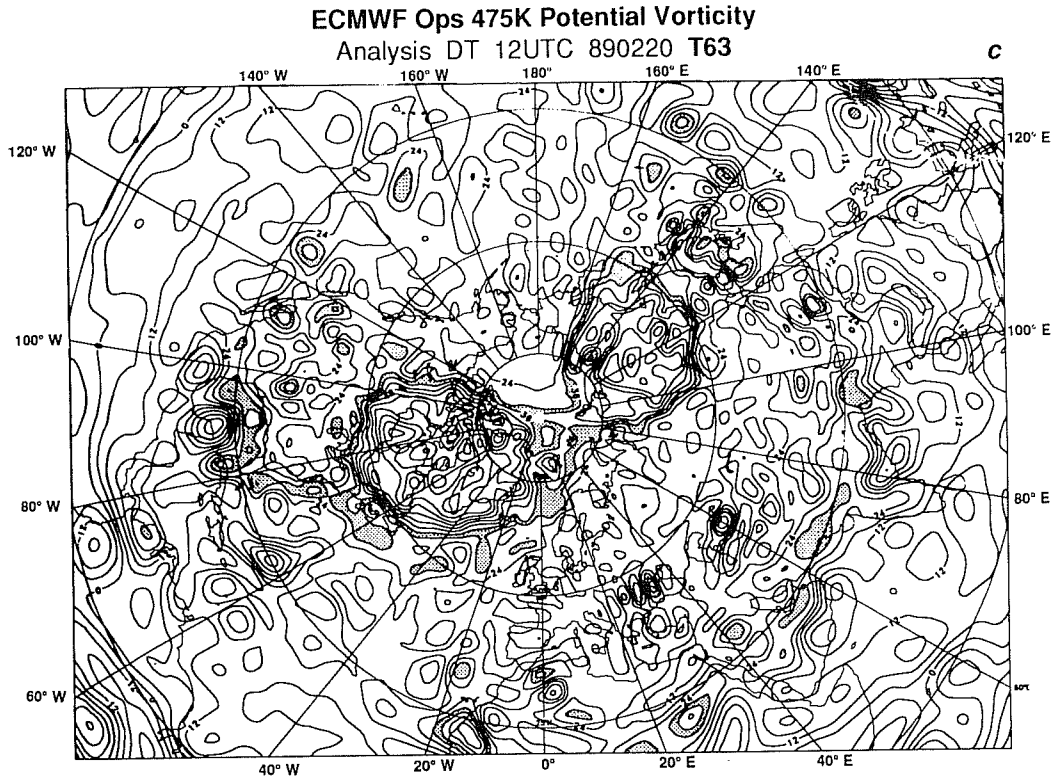

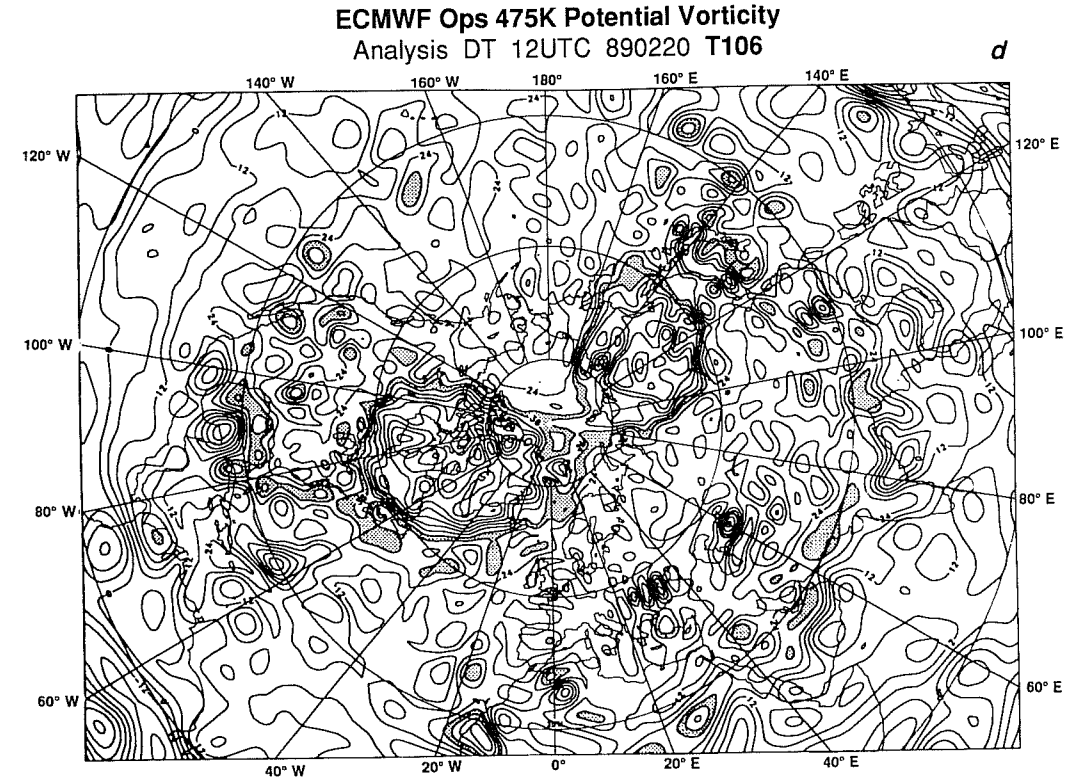

Fig 16 (continued).

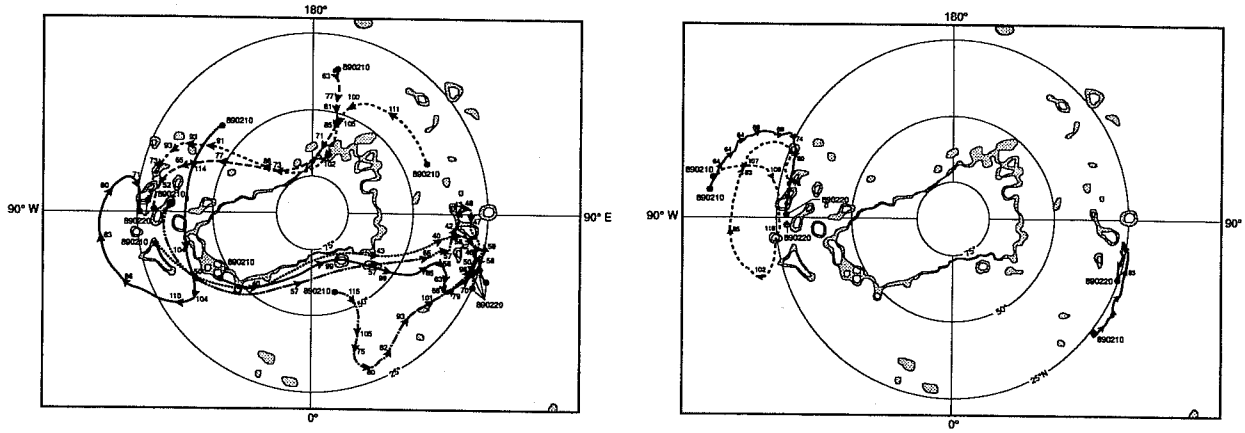

a b

Fig 17 10-day back trajectories (a) from low latitude, low PV air surrounding ex-vortex blobs, (b) from high PV air in low latitudes. The air parcels in (a) are always at low latitudes, while the parcels in (b) were at the vortex edge during the previous 10 days.

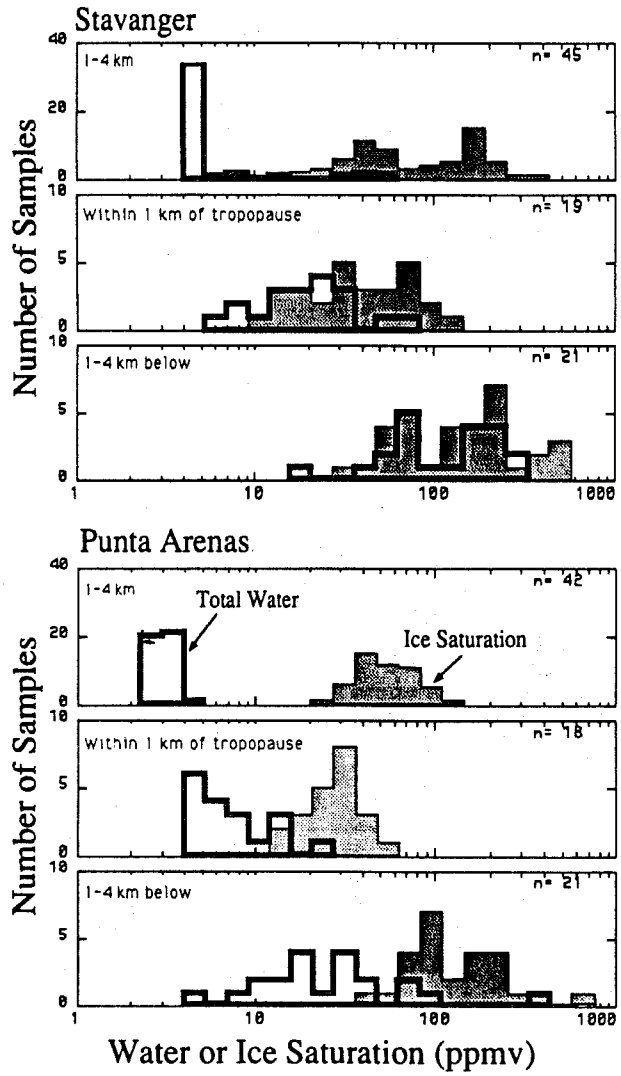

Fig 18 Histogram of total water mixing ratio (open, heavy outline) and ice saturation mixing ratio (shaded, thin outline). Legends in the top left corner of each box give location with respect to the tropopause. The top box is above the tropopause in each case. Saturation was frequent over Stavanger, but was not observed over Punta Arenas.

drier than its Northern counterpart during boreal winter. The only explanation so far offered for this asymmetry is that dehydration occurs during the June - September period in the Antarctic vortex, and that this dehydration is spread throughout the Southern Hemisphere lower stratosphere by the end of this period (*Tuck, Russell & Harries,* 1993). Figure 19 illustrates this effect; the signature of Antarctic dehydration affects the values of D over the entire Southern Hemisphere below 10 hPa, with values < 6·0 ppmv well outside the vortex, whose edge is statistically at about 65°S, but which extended occasionally to 45°S during the period considered. Figure 20 shows orthographic projections of methane values at selected levels, two for the Northern Hemisphere, one for the Southern. All show the peel-off of low methane from the polar vortex, with tongues of such air over the northern subtropical continents.

One interesting result is that the HALOE view of the Antarctic vortex is readily and obviously compatible with the ECMWF wind fields, but much less so with the equivalent PV fields (*Russell et al.,* 1993b). Figure 21a shows the ECMWF 30 hPa wind field for 911022, with the 15 HALOE observations marked as crosses. All the observations are within the vortex in the sense that they are poleward of the axis of the polar night jet stream. Further, it may be seen that there is an area of zero and near-zero winds, centered off the pole at the base of the Antarctic Peninsula, at about 75°S, 60°W. The HALOE observations are very well correlated with this structure; the methane profile has a constant mixing ratio from the stratopause down to about 30 hPa at this location, indicating unmixed descent from about 1 hPa. The methane increases radially outwards from the centre of the vortex - the point of zero winds - towards the jet axis (Figure 22). There is clear evidence that air with midlatitude characteristics has penetrated the vortex but neither this or the presence of a vortex center with unmixed descent could be deduced from the PV map (Figure 21b). The UKMO UARS PV analysis at Θ = 850 K for the day (Figure 23) does show low PV poleward of the jet axis at about 78°S, 160°E, the location of the high methane intrusions. The region of near zero winds is also characterized by a region of high absolute PV, consistent with the unmixed descent and low methane values. The lack of consistency of the ECMWF PV values may be the result of proximity to the uppermost level of the model (10 hPa); the UKMO-UARS analysis extends to 1 hPa, and moreover is specifically designed for stratospheric retrievals.

6. CONCLUSIONS

The ER-2 and HALOE both show evidence that Antarctic dehydration, thermodynamically possible inside the lower stratospheric vortex from early June to early October, spreads throughout the Southern Hemisphere by the end of this period. Vertical aircraft profiles at the core of the polar night jet reveal pronounced laminar structure in wind speed and direction, nitrous oxide, water vapour, ozone and chemically reactive species. Horizontal flight tracks reveal filaments off ex-vortex air equatorward of the jet axis. ER-2 observations in the tropics during boreal winter reveal an adequately cold tropopause at Darwin, co-incident with a minimum in total water, suggesting that this is indeed where air enters the stratosphere; a continental scale anticyclone at 100 hPa over Australia appears to play a key role in adiabatically cooling large masses of air to the requisite temperatures. The upper tropical troposphere on the northern flank of

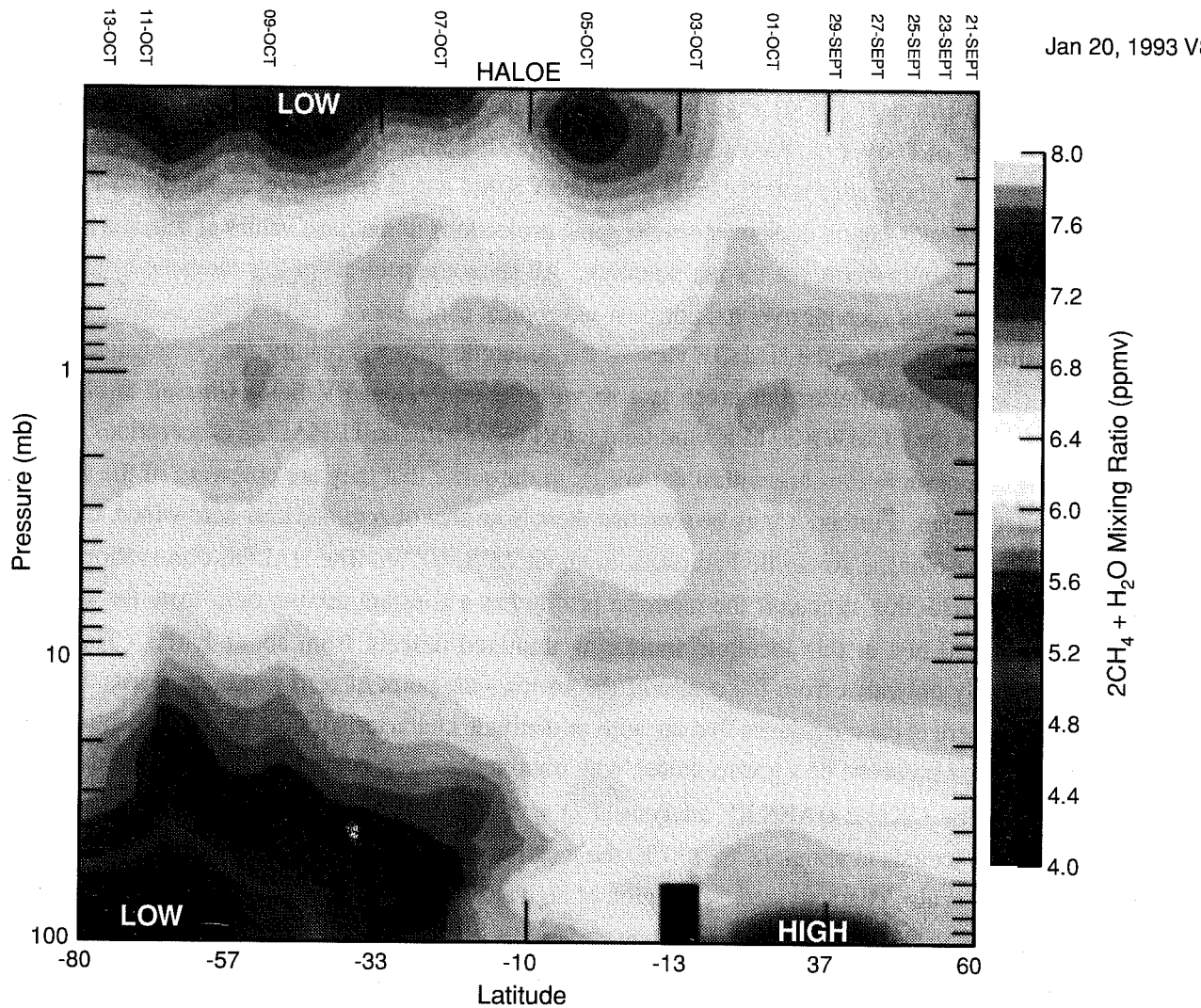

$2CH_4 + H_2O$ Pressure vs. Latitude Cross Section, Sunset on 21-SEP to 15-OCT 1992

Fig 19 A cross-section of D = 2 *CH_4 + H_2O. There are 15 sunset profiles every day in this picture; the latitude of every other day is marked at the top. The values of D less than 6·4 ppmv signal dehydration by ice crystal sedimentation at temperatures lower than that of the tropical tropopause, in the Antarctic winter vortex. The values of D in the southern lower stratosphere are somewhate lower in this retrieval (V8) than those in later, improved versions (V14 and later), but the new retrievals still show the inter-hemispheric asymmetry consistent with the ER2 observations in fig 6.

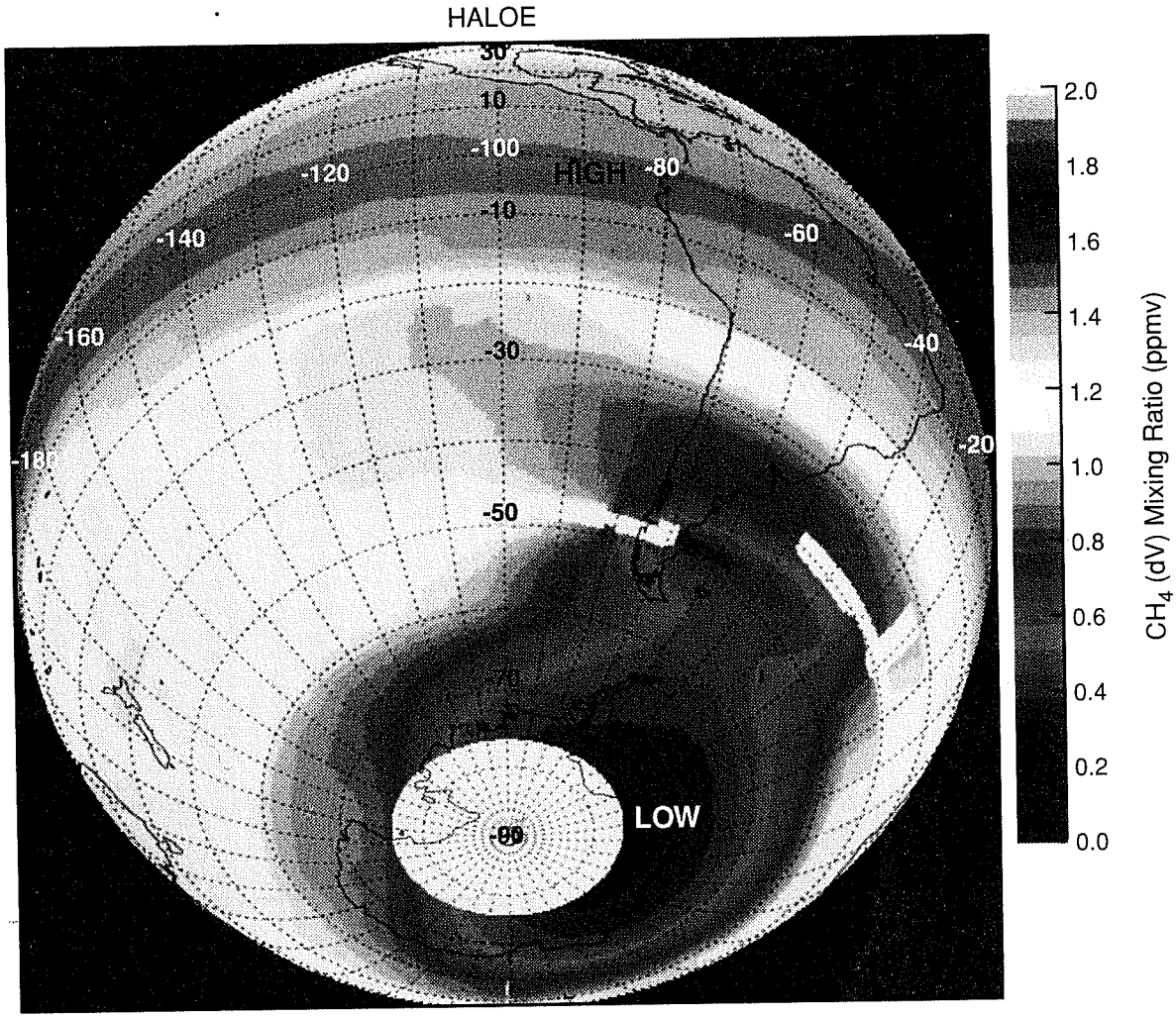

CH_4 (dV) 560.0 K Surface Cross Section,
Sunrise on 21-SEP to 15-OCT 1992

Fig 20(a) Orthographic projections of methane, spring, V8 retrievals, Southern Hemisphere, Θ = 560 K.

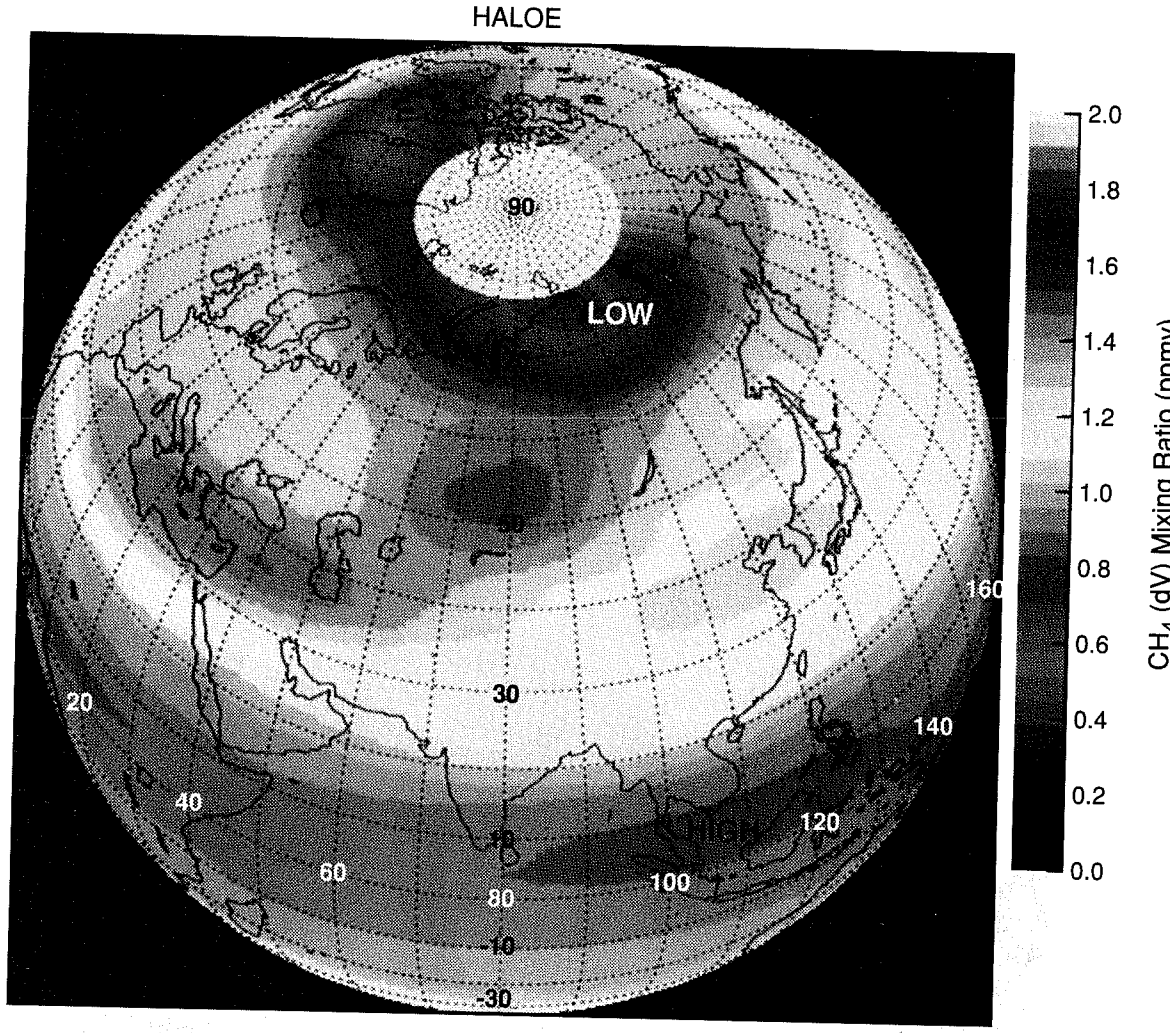

CH_4 (dV) 38.3 mb Surface Cross Section, Sunrise on 05-MAR to 11-APR 1993

Fig 20(b) Northern Hemisphere, 38·3 hPa, eastern hemisphere.

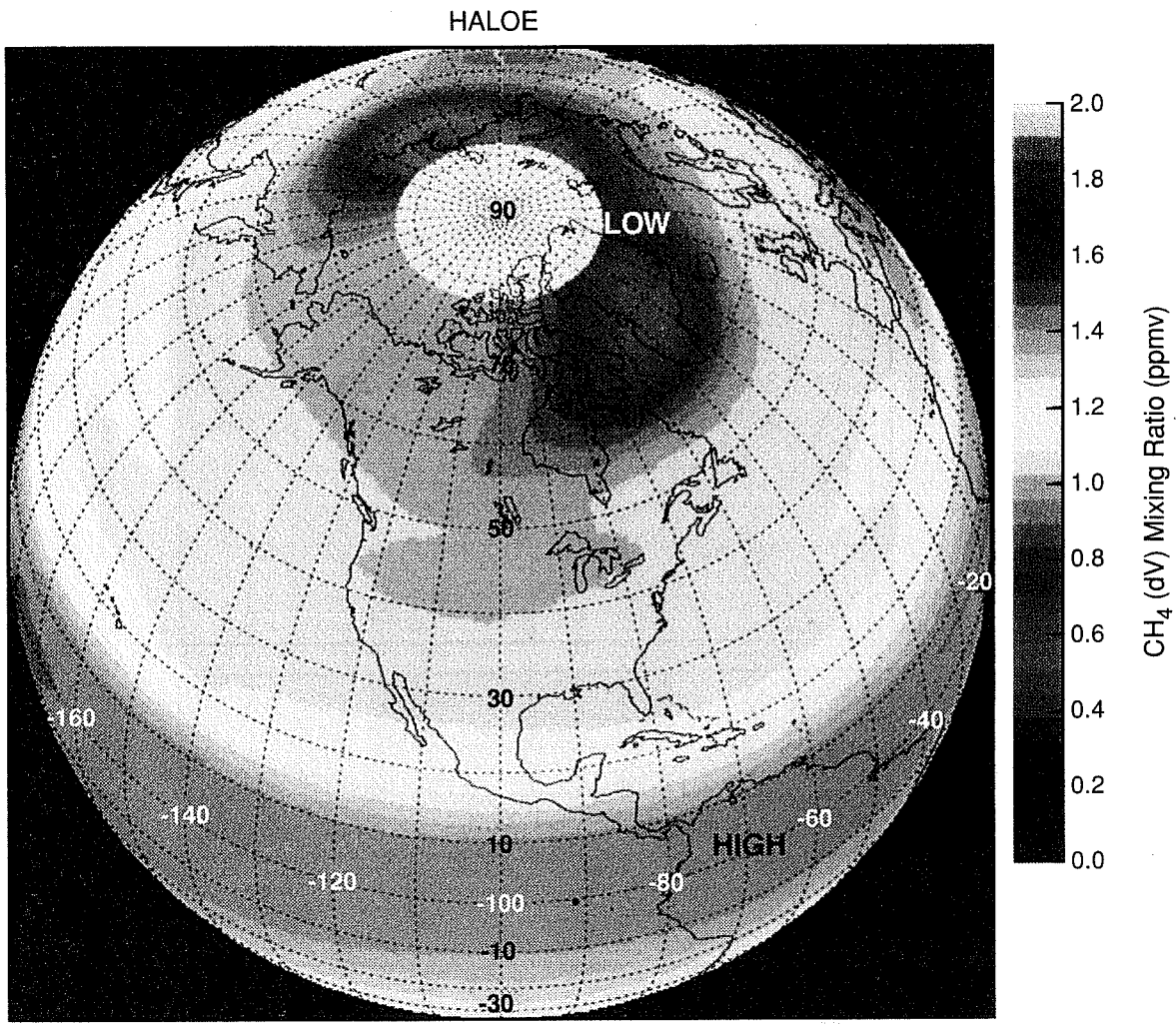

CH_4 (dV) 38.3 mb Surface Cross Section, Sunrise on 05-MAR to 11-APR 1993

Fig 20(c) Northern Hemisphere, 38·3 hPa, western hemisphere. The 24-day period of the observations includes some vortex motion as a bias, but there is clear evidence of the peel off of air from the vortex edge in all 3 cases, to latitudes of 20° - 30° over the Mediterranean and west of Chile.

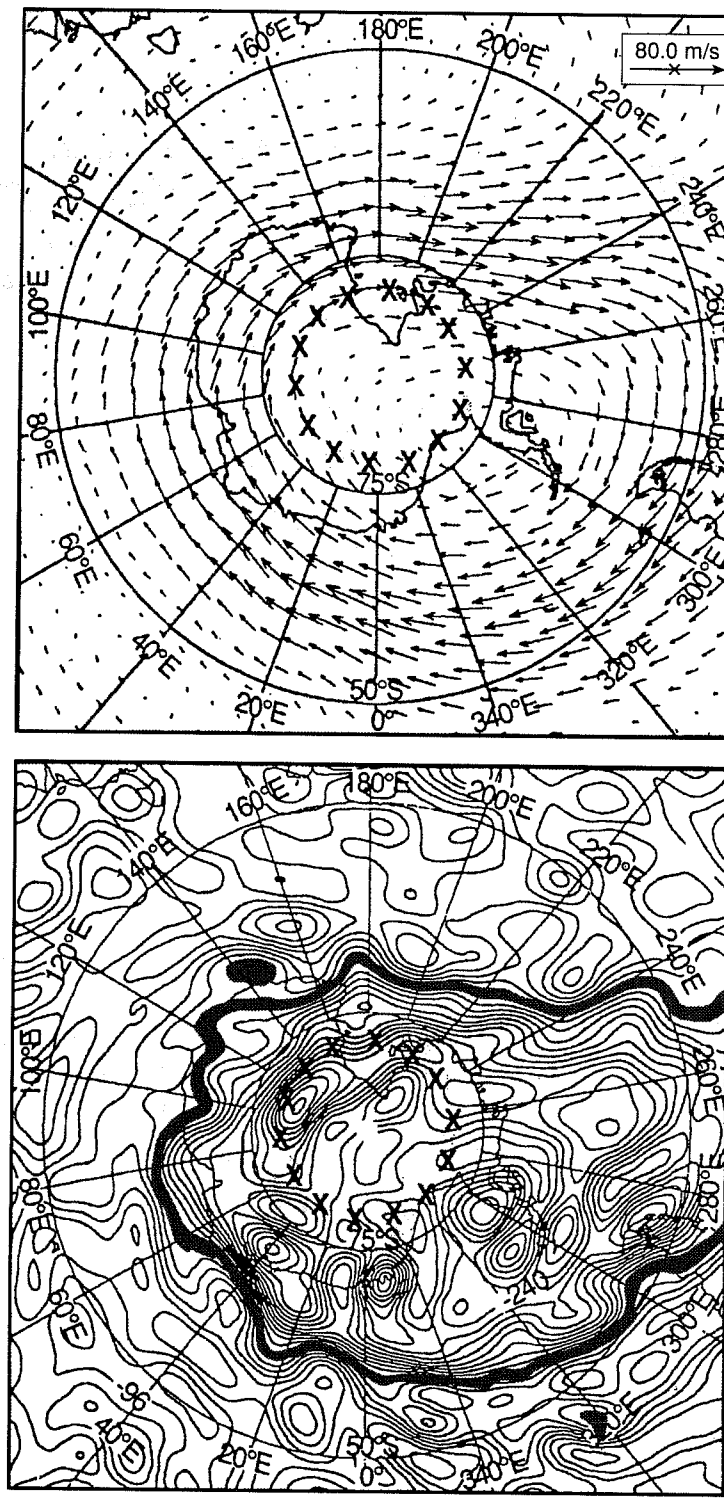

Fig 21 (a) ECMWF 30 hPa wind field 911022, with the 15 HALOE observations marked by crosses. All are poleward of the axis of the polar night jet stream, ie. they are inside the vortex. (b) shows the Θ = 700 K PV map for the same day; the HALOE observations are well inside the tightest PV gradient.

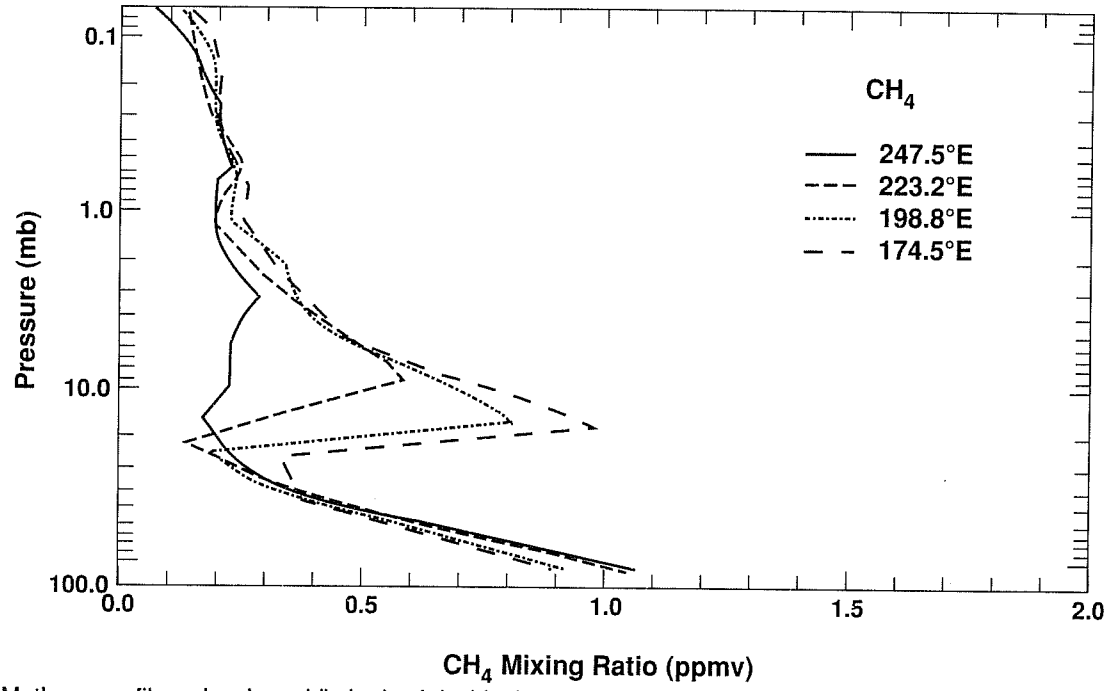

Fig 22 Methane profiles, showing midlatitude air inside the vortex between 3 and 30 hPa on 911022, the day of the ECMWF maps in fig 21. Fig 21 makes it clear that these profiles are inside the vortex. There is no correlation between these profiles and the ECMWF PV map of fig 21b, although the point of zero winds in fig 21a is accurately co-located with the profile indicating unmixed descent from the stratopause, at ~ 250°E, the base of the Antarctic peninsula.

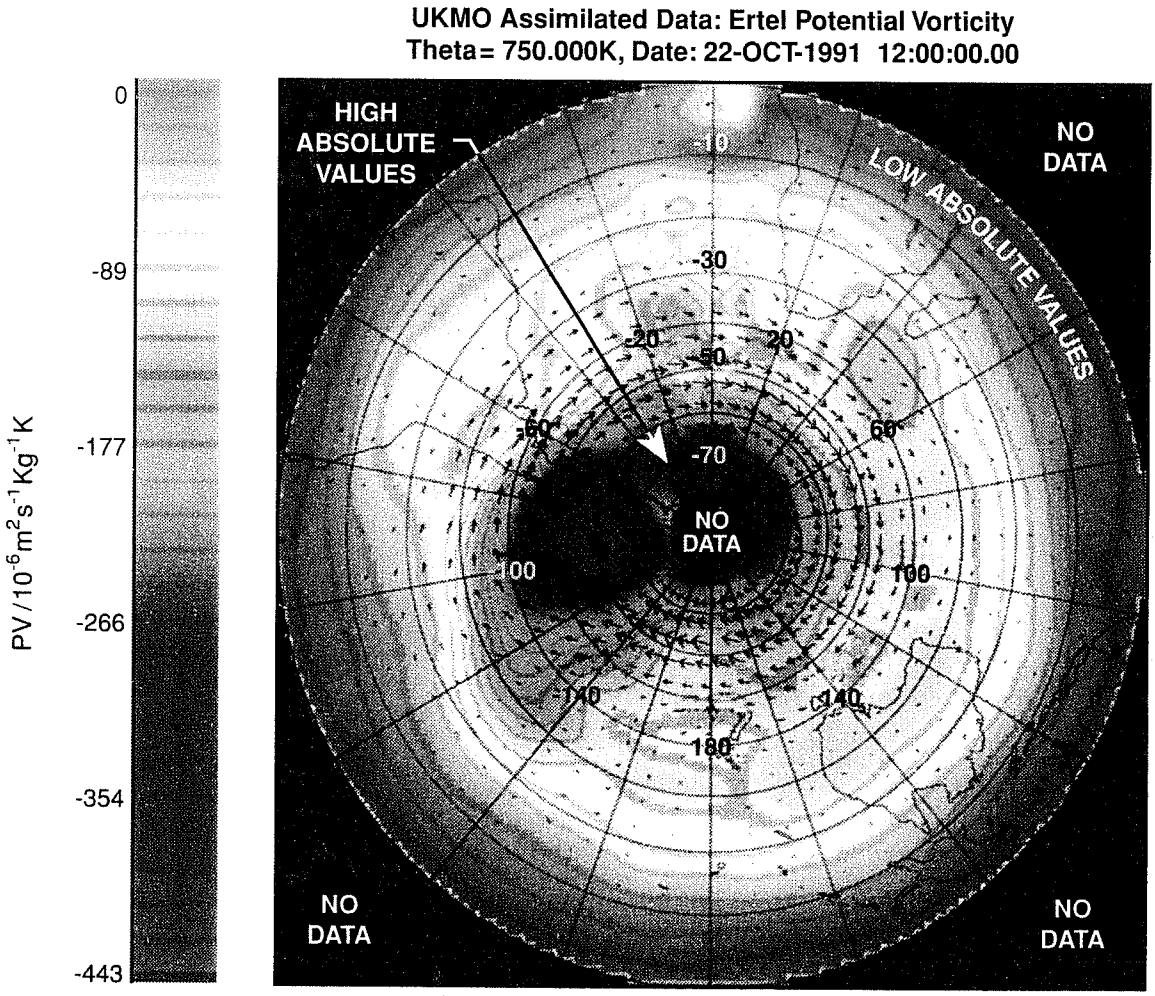

Fig 23 UKMO/UARS PV analysis at Θ = 850 K, 911022, the same day as figures 21 and 22. The low PV values from 220°E (140°W) to 140°E at 77°S (the HALOE lat), correspond to the intrusions of midlatitude air in fig 21b. They are well poleward of the jet axis, and so are inside the vortex. Note also the high absolute values of PV between S. America and the Antarctic peninsula, consistent with the unmixed descent in the profile at 247·5°E (112·5°W).

this anticyclone was frequently saturated, with large numbers of small ice crystals present.

Although not specifically designed for stratospheric analysis and forecasting, the ECMWF products show many features consistent with airborne and satellite observations. The operational forecasts of the location of the vortex edge were good, as were the winds and temperatures along aircraft tracks with a few exceptions. There were some occurrences where the forecasts and analyses did not accord with reality:

(i) The amplitudes (poleward extent) wind speeds of upper tropospheric/lower stratospheric ridges over W. Antarctica were underestimated, and the temperatures overestimated (Figure 10).

(ii) The minimum temperatures at the tropical tropopause were overestimated, by 3-7 degrees C. This difference is critical for understanding the dryness of the stratosphere (Figures 3, 4).

(iii) The fine scale filamentation of vortex air into mid-latitudes was not reproduced at all by the T + 24, T63 forecasts, and was under-represented by both T63 and T106 analyses (Figures 15, 16).

(iv) The PV analyses did not correlate well with tracer observations by satellite in the Antarctic vortex (Figures 21-23). This was not true of the wind field, and may be a result of proximity to the upper level in the model/analysis system.

7. ACKNOWLEDGEMENTS

The cooperation of ECMWF staff during the observational campaigns described here is greatly appreciated. Such field missions involve many people, and the author owes a very large debt to the Science Teams of STEP, AAOE, AASE, and HALOE. The ER-2 water vapour data displayed here are due to Ken Kelly, and the meteorological variables are due to Roland Chan. Jim Russell is the principal investigator of the HALOE instruments.

8. REFERENCES

Danielsen, E. F., In situ evidence of rapid, vertical, irreversible transport of lower tropospheric air into the lower tropical stratosphere by convective cloud turrents and by larger scale upwelling in tropical cyclones. *J. Geophys. Res., 98,* 8665 - 8682, 1993.

Kelly, K. K., M. H. Proffitt, K. R. Chan, M. Loewenstein, J. R. Podolske, S. E. Strahan, J. C. Wilson, and D. Kley, Water vapor and cloud water measurements over Darwin during the STEP 1987 Tropical mission, *J. Geophys. Res., 98,* 8713 - 8724, 1993.

Kelly, K. K., A. F. Tuck, D. M. Murphy, M. H. Proffitt, D. W. Fahey, R. L. Jones, D. S. McKenna, M. Loewenstein, J. R. Podolske, S. E. Strahan, G. V. Ferry, K. R. Chan, J. F. Vedder, G. R. Gregory, W. D. Hypes, M. P. McCormick, E. V. Browell, and L. E. Heidt, Dehydration in the lower Antarctic stratosphere during late winter and early spring, 1987, *J. Geophys. Res., 94,* 11317 - 11358, 1989.

Kelly, K. K., A. F. Tuck, L. E. Heidt, M. Loewenstein, J. R. Podolske, S. E. Strahan, and J. F. Vedder, *Geophys. Res. Lett., 17,* 465 - 468, 1990.

McKenna, D. S., R. L. Jones, J. Austin, E. V. Browell, M. P. McCormick, A. J. Krueger, and A. F. Tuck, Diagnostic studies of the Antarctic vortex during the 1987 Airborne Antarctic Ozone Experiment: Ozone miniholes, *J. Geophys. Res., 94,* 11,641 - 11,668, 1989.

Murphy, D. M., K. K. Kelly, A. F. Tuck, M. H. Proffitt, and S. Kinne, Ice saturation at the tropopause

observed from the ER-2 aircraft, *Geophys. Res. Lett., 17,* 353 - 356, 1990.

Russell, J. M., III, A. F. Tuck, L. L. Gordley, J. H. Park, S. R. Drayson, J. E. Harries, R. J. Cicerone, and P. J. Crutzen, HALOE Antarctic observations in the spring of 1991, *Geophys. Res. Lett., 20,* 719 - 722, 1993.

Salter, P. R. S., and S. D. Merrick, A note on forecasting for the Airborne Antarctic Ozone Experiment, *Met. Mag., 118,* 59 - 63, 1989.

Tuck, A. F., J. M. Russell III, and J. E. Harries, Stratospheric dryness: antiphased desiccation over Micronesia and Antarctica, *Geophys. Res. Lett., 20,* 1227 - 1230, 1993.

Tuck, A. F., Synoptic and chemical evolution of the Antarctic vortex in later winter and early spring of 1987. *J. Geophys. Res., 94,* 11,687 - 11,737, 1989.

Tuck, A. F., et al., Polar stratospheric cloud processed air and potential vorticity in the northern hemisphere lower stratosphere at midlatitudes during winter, *J. Geophys. Res., 97,* 7883 - 7904, 1992.